Technical report; TR 228

KNMI

Evaluation of modified soil parameterization in the ECMWF landsurface scheme

R.J.M. IJpelaar

Koninklijk Nederlands Meteorologisch Instituut

De Bilt, 2000

Technical report = Technisch rapport; TR-228

De Bilt, 2000

PO Box 201
3730 AE De Bilt
Wilhelminalaan 10
Telephone +31 30 220 69 11
Telefax +31 30 221 04 07

Author: R.J.M. IJpelaar

UDC: 551.509.313
551.509.51
551.588.3

ISSN: 0169-1708

ISBN: 90-369-2182-1

Evaluation of modified soil parameterization in the ECMWF landsurface scheme

(Final thesis "Meteorology" Wageningen University)

author:
R.J.M. IJpelaar

Supervisors:
B.J.J.M. van den Hurk (KNMI)
M. Soet (Alterra and Wageningen University)

Participating organizations:
KNMI dep. Climate Research & Seismology, division Atmospheric Research
Alterra SC-DLO dep. "Water and the Environment"
Wageningen University: subdep. "Meteorology and Air Quality", and "Water Resources"

Summary

In regional climate models, exchange of energy and water between the land surface and the atmospheric boundary layer is calculated by Land Surface Parameterization (LSP) schemes. The water balance in the soil system – distribution of precipitation over soil water, runoff and evapotranspiration - influences those surface fluxes and plays an important role in the land part of the hydrological cycle. Soil hydraulic properties, as hydraulic conductivity and water storage capacity, determine the amount and distribution of soil water and eventually the partitioning of runoff and evapotranspiration. Recent research focusses on improving the representation of the seasonal hydrological cycle. Adequate parameterization of soil water is crucial to achieve this goal.
In the current version of TESSEL (Tiled ECMWF Surface Scheme for Exchange processes over Land), soil hydraulic properties are based on the Clapp and Hornberger (CH) soil parameterization, and are uniform for all gridpoints of the host atmospheric model. Aim of this research is to evaluate the implementation of a variable soil map, based on Mualem-van Genuchten (MVG) parameterization in TESSEL for the dry European summer in 1995. Each gridpoint now has a specific soil type, ranging from "coarse" (sand) to "very fine" (clay). The KNMI atmospheric research model RACMO is used on a 50 km resolution grid over Europe.
Several regional study areas, based on the soil type, have been selected. This selection is supported by an analysis of the European climate elements "temperature" and "precipitation" and their consequences for the soil water regime. For each of the dominant soil types "coarse" and "medium", wet and dry study areas could be distinguished.
The first part of the research comprises analysis of changes in soil water balance terms "precipitation", "runoff", "evapotranspiration" and "change of soil water storage" between the control (CH) model run and the modified (MVG) model run. Larger soil water storage capacity and smaller hydraulic conductivity for most (MVG) soil types cause evapotranspiration and precipitation to increase for the mainland of Europe in summer. Surface runoff occurs more often, while deep runoff has decreased.
The second research question addresses the comparison of the modelled and observed relative humidity at 2 m level. Shifts of evapotranpiration between the MVG and CH run are expected to correlate with changes in relative humidity. The unbiased RMS has decreased for the whole simulation period, while model bias indicates a model decline for spring and improval for summer.

Details about the changes in water balance and relative humidity for each soil type are summarized in Table 6.1 of this report. The variable soil map with MVG parameterization causes shifts in the modelled water balance, although they are small. A division between coarse soil types with relative large hydraulic conductivity and low evapotranspiration, and all other fine soil types with smaller hydraulic conductivity and large soil water storage capacity leading to higher evapotranspiration, can be made.

Contents

Chapter 1 Introduction

"Gaea (Earth) and Uranos (Heaven) are both half-parts of the Oerei (total world) that developed from Nyx (Night or Chaos) and from which appeared Eroos (desire for love). Gaea became an active basic principle in the cosmos of Hesiodos, together with Chaoos and Eroos. She was the mother and wife of 'Father' Uranus. They were the parents of the first creatures, the Titans, the Cyclopes, and the Giants - the Hecatoncheires (Hundred - Headed Ones). Uranus hated the monsters, and, even though they were his children, locked them in a secret place in the earth. Gaea was enraged at this favoritism and persuaded their son Cronos to overthrow his father. He emasculated Uranus, and from his blood Gaea brought forth the three avenging goddesses the Erinyes. Her last and most terrifying offspring was Typhon, a 100-headed monster, who, although conquered by the god Zeus, was believed to spew forth the molten lava flows of Mount Etna. Mother Gaea, however, was the protection of human life against the selfishness of the male element: Uranos and Cronos (Time), the son of Uranos" (sources: http://www.ancientgreece.com and Encyclopedia Brittanica).

Almost nothing is more complex as 'Mother Gaea', the Ancient Greek word for the personification of planet Earth. In the modern world, Gaea has the global meaning of the interactive system Earth which is formed by the Atmosphere, Hydrosphere, Lithosphere (solid earth), Biosphere and Cryosphere (solid water).

Nobody can deny the enormous entanglement of these components and their complex behaviour in climate and weather. Since beginning of human civilisation, man tries to unravel mysteries of nature. Research fields as Meteorology, Hydrology, Biology, Chemistry and Geology were born, as tools to satisfy our desire for knowledge.
Today, most problems are quite clear for most disciplines *separately*. We know e.g. how air behaves for certain temperature-gradients and we know how water finds its way in the soil for certain boundary conditions. One big challenge has still to be taken up: understanding the exact interaction and feedback of the climate's systems.
This can only be achieved by repeatedly developing and modification models and doing high quality field measurements. In this research, attention is paid to the role of soils in the Hydrosphere and the interaction to the Atmosphere in seasonal climate in Europe.

1.1 Aims en scientific questions

Land use is very important for climate and long-term weather models, because it stongly influences the processes at the land surface which forms the link between the hydrological cycle at land and in the atmosphere. Land use mainly includes human related matters like agriculture, industry, infrastructure. Today, they influence the land surface properties at most, especially in areas with dense population. But also natural activities - often deduced from human activities - like forest fires, land erosion, avelanches determine land surface properties. Sound upscaling and averaging from small scale and short-time processes to larger scales in climate and long-term weather models is crucial. The soil moisture reservoir plays an important role in this, because it has a huge storage capacity for water and energy and acts as a filter for (noisy) small scale and short-time processes.

Soil moisture and the soil water balance are affected by **atmospheric elements** (precipitation, solar radiation, temperature) and **soil hydraulic properties**.
In chapter 2, long-term averages of the atmospheric elements (climatological elements) and their influence on soil moisture are briefly discussed. **Most attention** in this research is paid to the soil hydraulic properties (chapter 3), which involve e.g. the hydraulic conductivity, diffusivity, and water-retentitivity curves of soils, and play a key factor for soil water budget terms like runoff, bare soil

evaporation, transpiration, drainage and storage. Figure 1.1 shows the land part of the hydrological cycle and illustrates the discussion above.

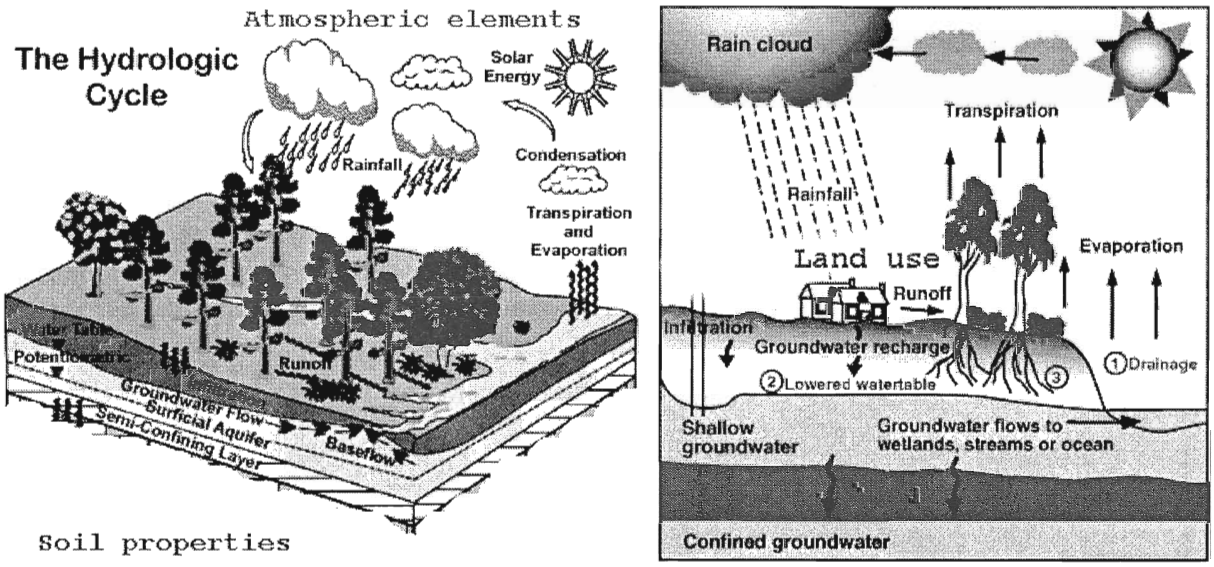

Figure 1.1 Land part of hydrological cycle and atmospheric and soil hydraulic elements

There are many interactions between the atmospheric element and the soil hydraulic properties. In West Europe for example, is precipitation highly correlated to the western circulation, so signals from the Atlantic Ocean are predominant. But sometimes, especially in summer, there is no strong western circulation, and precipitation is regenerated from local evapotranspiration. Interesting issue here is to determine which part of the precipitation originates from land evapotranspiration and which part from seawater. The behaviour of the evapotranspiration is determined by the soil hydraulic properties, mainly the storage capacity of the soil reservoir. So the land-surface on its turn can change the climatic elements.

For a proper representation of the interaction between the physical and biological processes in the upper layer of the earth's surface and the boundary layer of the atmosphere in Numerical Weather Prediction Models (NWP's) and Global Climate Models (GCM's), landsurface parameterization schemes (LSP-schemes) have been developed. They are the most appropriate tools to investigate long-term effects of soil-moisture on seasonal climate and vice versa.
The basic physics of a soil can be represented by the one-dimensional conservation equations for temperature and water content. The main task of a LSP-scheme is to solve this equation system for a particular soil layer configuration and to provide the necessary boundary conditions - based on conceptual assumptions - for the soil system, like the relation between soil moisture and the hydrological fluxes. Many more physical and biological elements of the land surface, like snow, vegetation and planetary boundary-layer representation are parameterized (vdHurk et al., 2000), but these will not be discussed extensively in this report.
GCM's necessarily operate on a coarse spatial resolution (see Chapter 3 for more information about temporal and spatial scales). The study of Europe needed finer model resolution, so regional forecast and climate models such as HIRLAM (Gustafsson, 1993), RACMO (Christensen et al., 1996) and REMO (Jacob et al., 1997) - developed to allow regional analyses of weather and climate systems- are very useful for this purpose.
The roots of this research are embedded in the aims of a project of the National Research Programme on Global Air Pollution and Climate Change, called NRP. The NRP is a strategic research programme for the encouragement and financing of climate research, conducted by a variety of universities and

institutions: more than 30 Dutch research institutes are working on problems that, directly or indirectly, have to do with 'global change' and climate change[1]. In this project, the Department of Meteorology and Air Quality and that of Water Resources of Wageningen University, The Royal Dutch Meteorological Institute (KNMI) and Alterra are involved. The aims of that project are:

* Understanding the causes of excessive drying over the European continental area in the large scale climate and weather forecast models

* Improving the representation of the seasonal hydrological cycle in climate and weather forecast models

In order to meet these goals, Alterra (formerly DLO Winand Staring Centre) played an active role in constructing a soil-texture data base for Europe. Wösten et al., (1999) presented the HYPRES (Hydraulic Properties of European Soils) data base, that supplies **Mualem-van Genuchten (MVG)** parameters (for more details, see § 3.3) for 5 soil-textures and histosols of the well-known FOA soils type map. This can be linked to mapping units for mesoscale models, resulting in a **variable field** soil map for Europe. Each gridpoint has thus its own soil texture value. This is implemented in the Regional Atmospheric Climate Model (RACMO), which is a research model of the KNMI for climate and long-term weather studies. RACMO uses TESSEL (Tiled ECMWF Surface Scheme for Exchange processes over Land) (Viterbo et. al., 2000 in press) with a **constant** soil-texture field and the soil hydraulic properties based on **Clapp and Hornberger (CH)** parameterization (1978). This is a three dimensional configuration, because the dynamics of the air are taken into account. TESSEL has been implemented as part of the ERA-40 (ECMWF Reanalysis 1957-2001) project. The central **aim** of this research is to verify if the HYPRES data base is improving the settings of soil hydraulic parameters for TESSEL. Formulated more in detail:

Does implementation of a variable Mualem van Genuchten soil parameterization, replacing the non-variable Clapp and Hornberger soil-type in TESSEL, has a significant and beneficial effect on the model results of RACMO, related to the land surface branch of the hydrological cycle for a dry summer season (1995) in Europe?

Deduced from this, there are two core sub-issues that comprise more or less the strategy of this reseach:

1. What is the behaviour of the **water balance** for several study areas with different soil characteristics in Europe? (Chapter 4). Is there some influence on the soil hydrology budget terms in the RACMO-output, i.e. the distribution of precipitation among the runoff (drainage, interflow and surface runoff), evapotranspiration and soil-storage? This is evaluated by comparing the current TESSEL model (CH) and the modified TESSEL model (MVG)
2. How does the observed **relative humidity** compare to the RACMO results for the Clapp and Hornberger versus the Mualem van Genuchten soil parameterization, and can this be checked in a statistical sound way by analyzing the bias and unbiased RMS (Chapter 5)? The relative humidity indicates the link between the water- and surface energy balance: the evapotranspiration.

[1] For the main strategy of the NRP,see the website: http://www.nop.nl

1.2 Overview recent research

Before we discuss the present state of the LSP-schemes and some limitations of them, a basic overview of several schemes in last decennia will be presented. A specialised research program is PILPS[2] (Project for Intercomparison of Landsurface Parameterization Schemes), which has the aim to improve our understanding of the parameterization of interactions between the atmosphere and the continental surface in climate and weather forecast models (Henderson-Sellers et al., 1993).
PILPS is a World Climate Research Programme project operating under the auspices of GEWEX (Global Energy and Water Cycle Experiment) and WCRP (World Climate Research Programme). It has been designed to be an on-going project. Since its establishment in 1992, PILPS has been responsible for a series of complementary experiments, with focuses on identifying parameterization strengths and inadequacies. About 30 landsurface process modelling groups have been participating in PILPS.
The oldest and most simple model was a so-called bucket model (Manabe, 1969). In this model, one soil layer simply absorbs the water, until it becomes saturated. No drainage occurs, and runoff is simply the water determined by the excess of soil moisture above saturation level. Since then, more complexity was introduced in LSP-schemes: multiple soil and vegetation layers, drainage and subsurface flow, diffusion of water. According to their structure, LSP's have been developed and used for versatile purposes, varying from coarse gridded GCM's with few soil layers to highly detailed biological models with many layers and integration of the carbon-cycle. A full description of all models is too extensive for the purpose of this report (for more information, see website PILPS).

Let us focus now on some basic characteristics of the soil hydrology for the current LSP-schemes. For total runoff, there are two major types of the LSP-schemes: those keyed to values of intermediate soil water content (field capacity and/or wilting point) and others which relate soil moisture to key diffusive parameters as water potential and hydraulic conductivity by non-linear continuous functions (Wetzel et al., 1996). The single layer model ECHAM4 is an example of the first type (Dümenil and Todini, 1992) and the multi layer model from the ECMWF (Viterbo and Beljaars, 1995) of the second type. TESSEL, used in this research, is a modification of the ECMWF scheme.
In ECHAM4, the most important hydrological aspects are the single soil moisture reservoir, the dependence of (sub)surface runoff to the *partial* saturation of a gridbox, and the deep drainage term which is operated by the mean soil moisture content (W) and a drainage threshold (at 90 % of W_{max}) for the hydraulic conductivity. Significant deep runoff only occurs at near-saturation conditions. In terms of the surface energy balance, the system of equations is solved for the entire grid box, which results in a single grid box surface temperature.
In the ECMWF LSP-scheme, the hydrology is governed by simplified Richards' equations which are solved for 4 layers. Important parameters are the hydraulic conductivity and diffusivity which are determined by widely used Clapp and Hornberger (1978) parameterization. The hydraulic conductivity and diffusivity are given as function of soil moisture content. Field capacity and permanent wilting point are core values of soil moisture content in the configuration of these functions. The modified ECMWF LSP-scheme produces these functions for specific soil-textures: the so-called class Pedo Transfer Functions (Wösten et al., 1998) with Mualem van Genuchten parameterization (1980).
Further, the root extraction of water (transpiration), is also determined by the field capacity and permanent wilting point. At soil moisture content values above field capacity, plant roots can *potentially* evaporate at maximum level. Below permanent wilting point, there is no transpiration at all. Surface runoff only occurs when the net precipitation (throughfall) exceeds infiltration rate of the soil, which is almost never the case. The same can be stated for saturation runoff, which only occurs when a soil layer becomes supersaturated. The major contribution to runoff is deep runoff. This is evident for a wide range of soil moisture content. The energy fluxes of the surface are calculated apart for different tiles (subgrid surface fractions) in a gridbox, which leads to different surface temperatures (skin-temperature) and

[2] Many more information about PILPS can be found at the website: http://www.cic.mq.edu.au/pilps-rice

solutions for the surface energy balance. A more extensive description of the ECMWF LSP-scheme and recent modifications (TESSEL) can be found in Chapter 3.

Finally, it is worthwhile to mention a few shortcomings of the current models, related to their parameterization of soil hydraulic processes and properties and interaction to the atmosphere:

- An important conclusion of a study, which focussed on the modelling of liquid water fluxes of the vadose or unsaturated zone of the soil, is that most LSP-schemes underestimate the annual total runoff (runoff and drainage) and thus overestimate annual total evaporation (Wetzel et al., 1996).
- The ECMWF reanalysis for the Red-Arkansas River, carried out over the years 1985-93, revealed that the model compensates errors in the soil water balance by artificially supplying water for certain changes in specific humidity: nudging (Betts et al., 1998).
- The coupling between diurnal and longer time-scales processes is not adequate. The same ECMWF study (Betts et al., 1998) indicates that soil moisture (long time-scale) does not correlate well to precipitation, mixing ratio and boundary layer development (diurnal time-scales).
- One of the PILPS studies (Shao et. al., 1996) shows that it is difficult to compare all LSP-schemes, because they achieve different equilibrium states when forced with prescribed atmospheric conditions and that the time period to reach these states differs among schemes; and even when soil moisture is fairly well simulated, the processes (particularly evaporation and deep runoff) controlling the simulation differ among the schemes and at different times of the year.
- The parameterization of soil hydraulic properties is very simplified in comparison to the real behaviour of soils. Models produce errors in soil moisture content and hydraulic conductivity caused by ignoring factors as alternating wetting and drying of soils (hysteresis), orography, shallow groundwater tables, cracks in topsoils, swelling clay and other local soil irrigularities. This is mainly important for short time processes, but we can only assume that it doesn't affect seasonal time scales.
- Last but not least: the upscaling of small scaled processes to large gridpoints is not adequate. Parameters, such as the hydraulic conductivity of soils, are derived on field scale areas, but are now applied to large grids!

1.3 Setup report

In Chapter 2, some general background information is given for the seasonal characteristics of Western-Europe (for time period: 1920-1980). The development of the key climatological parameters, precipitation and temperature, can be compared to the climate values for the research time-interval (1995). The relevant technical aspects of the LSP-schemes of ECMWF (ECMWF version 1995 and modified TESSEL version) and their implementation in the host model RACMO will be discussed in Chapter 3. Included in the same chapter, the basics of soil hydraulic properties will be discussed. Chapter 4 analyses the partitioning of the terms precipitation, runoff, evapotranspiration and storage in the water budget for the specific areas based on soil-texture classification in Europe. In Chapter 5, the surface water and energy balances are linked, by analysing the relative humidity for the same study areas. A synthesis of the results of the sub-questions in the previous chapters is given in Chapter 6; conclusions and recommendations.

Chapter 2 Basic climatology of research area: Europe

Before the details of soil hydraulics and its relation to TESSEL (Tiled ECMWF Surface Scheme for Exchange processes over Land) will be discussed in chapter 3, general information about the current climate of Europe is discussed briefly in this chapter. Climatology - and especially that of Europe - is a very versatile and complex issue. Within the framework of this research, it is impossible to give an extensive analysis. But an overview of some basic climate characteristics over the last decades is useful, for two reasons:

- Simulation period in this research is 15 months. Seasonal weather of some areas in Europe may show extreme behaviour (temperature and precipitation anomalies), which is interesting for the analysis of the soil hydrology and relative humidity. Average values for temperature and precipitation are needed to recognize these regional anomalies.
- The selection of specific study areas in Europe (see § 4.2) is based on the soil texture. Soil moisture will probably be influenced by this soil-texture differences, but external climatological elements can not be disregarded of course. For two areas with the same soil-texture properties, but total different climates, it can be hard to distinguish common properties in the soil hydrology, based on soil-texture only. The results can be disturbed by climate elements, and it is important to recognize that.

There are three key-factors that are important for a general description of climate: **temperature**, **precipitation** and **solar radiation**. Other elements, like windspeed and atmospheric humidity at high altitudes play an important role too, but their observation records are often too short and inhomogeneous, which makes them less suitable for climate description (ECSN, 1995). Here, average seasonal temperature and precipitation will be emphasized, because those parameters are also used directly in the model-runs in this research. Implications of the basic climate characteristics in Europe for regional soil moisture will be discussed in the last paragraph.

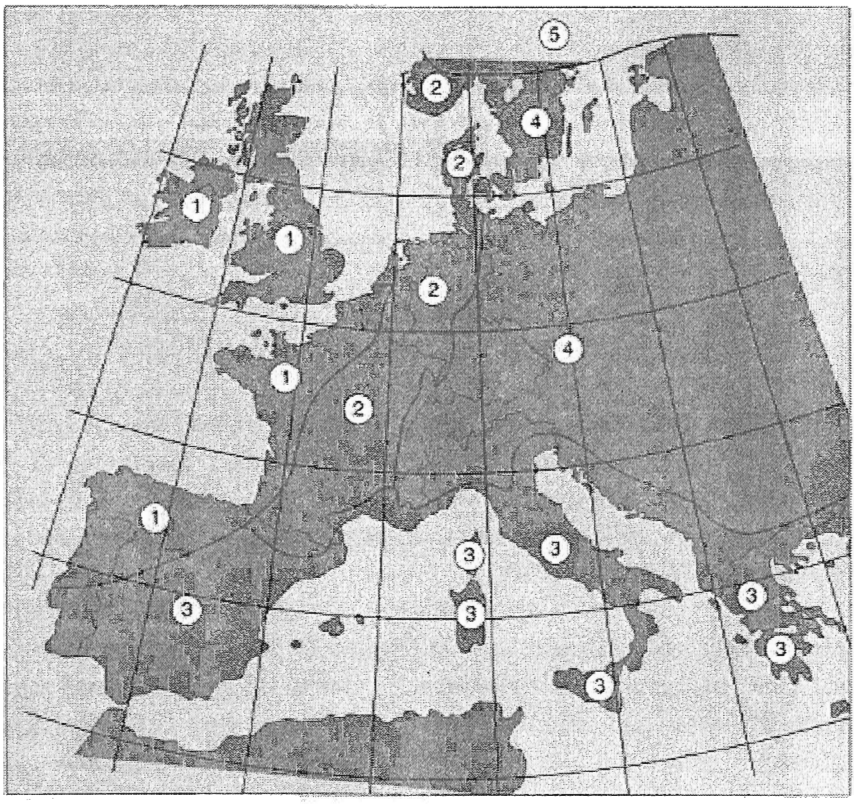

Figure 2.1 Areas according to the modified Köppen climate classification (ECSN, 1995)

2.1 General seasonal characteristics

Starting from the Köppen (1961) world classification of climates, Europe can be divided in two sharply contrasting parts. The zonal location of the main mountains chains (Pyrenees, Alps, Balcan Mountains) act as the boundary between Mediterranean climate type south, and the zone of temperate climates with a more or less pronounced continental influence north. Figure 2.1 shows a modified version of the Köppen classification, which is based on temperature criteria only (ECSN, 1995). The main modification in comparison to the original Köppen system is that the oceanic climate is further divided in a pure oceanic climate and an altered oceanic climate. There is also no classification for arid areas in Europe, based on precipitation, which comprise parts of Central and South Spain.

2.1.1 Temperature

As shown by the discussion about the Köppen classification, temperature mainly determines the climate types in Europe. To explore the seasonal climate, the criteria mentioned in Figure 2.1 are not sufficient. Figure 2.2 gives an overview of the mean surface air temperature for each season. The terrestrial data are derived from observations over 60 years (Legates and Willmott, 1990a).
The division of warm Mediterranean climate south and cooler climate types north of the mountain boundary line is distinct.

In winter and autumn the influence of the strong western flows is strong in South-West Europe, which is indicated by the isotherms curving far to the north. The continental climate in East Europe is demonstrated by the low temperatures (below 0° C) reaching towards the Balcan area. The Mediterranean area is relatively warm, but the differences in temperature compared to the rest of Europe are not as pronounced as in spring and summer.

The oceanic climate (area 1 in Figure 2.1) has no large amplitude in mean temperature, which causes relatively constant *potential* evapotranspiration (E_p) throughout the year. The evapotranspiration is the summation of bare soil evaporation and plant evaporation (transpiration). The altered oceanic climate (area 2) and continental climate (area 3) however, have relatively more E_p in summer than winter. The sub-arctic climate (area 5) has only temperatures above ca. 5° C in summer, so E_p is very small throughout the year. The mediterranean climate (area 4) has high E_p in all seasons, due to the overall high mean temperature. How much water actually can evaporate is, besides the incoming solar radiation which mainly determines the temperature, strongly dependent on the yearly amount and seasonal distribution of precipitation in each climate area.

2.1.2 Precipitation

The key input parameter for the soil hydrology is precipitation, which is distributed very inhomogeneous over Europe. Combined with the mean temperature, it provides the rough boundary conditions for the change of seasonal soil moisture content in the different climate areas in Europe. Figure 2.3 gives an overview of the mean precipitation for each season. These (terrestrial) data are, like temperature, derived from observations over 60 years (Legates and Willmott, 1990b).

Mountain areas receive more precipitation in general due to the uplifting of air masses and the following condensation of water vapour, especially at the windward side of the mountains. The mountains at the Atlantic shoares receive systematically more rain than the inland areas eastwards. The Alps have relatively much precipitation in summer, when warm humid air masses from the Mediterranean See collide with the southern hills. The mainland of Europe north of the Alps has significantly more precipitation in summer than in winter, due to heating of air. This convective precipitation, however, is very inhomogeneous

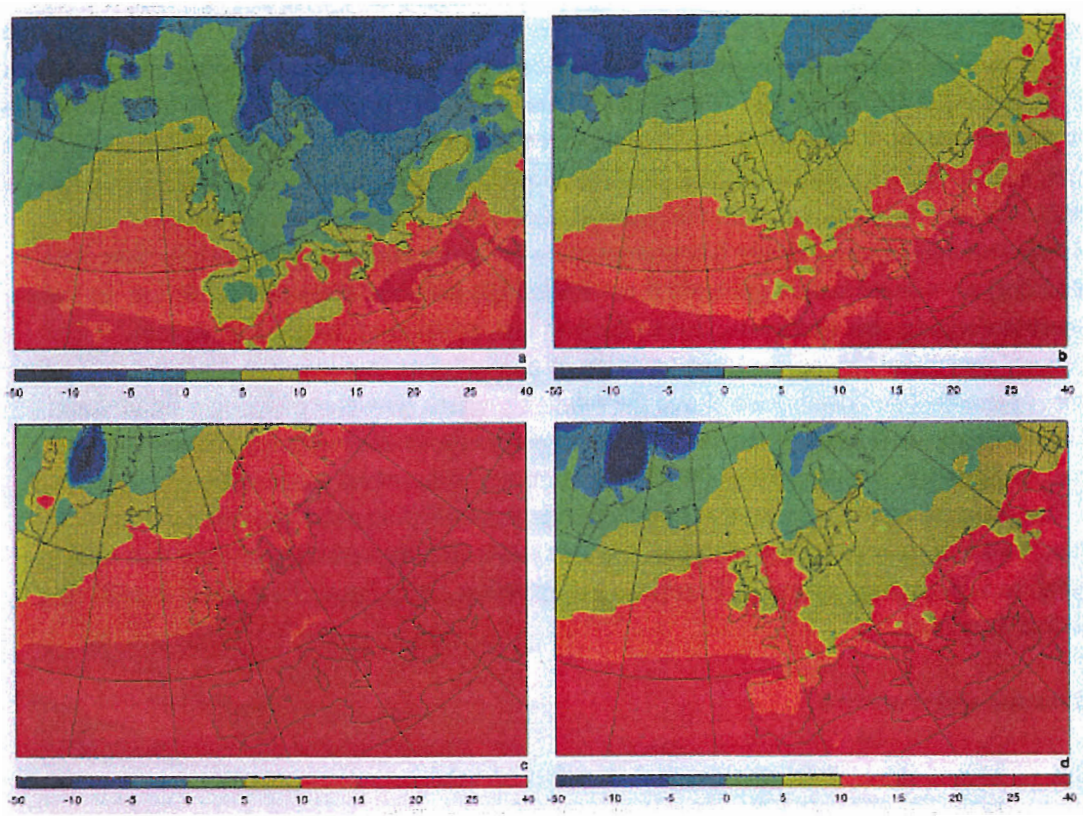

Figure 2.2 Mean surface air temperature for winter (a), spring (b), summer (c) and autumn (d). Terrestrial data time period is 1920-1980, oceanic ship data: 1950-1972 (Legates and Willmott., 1990a)

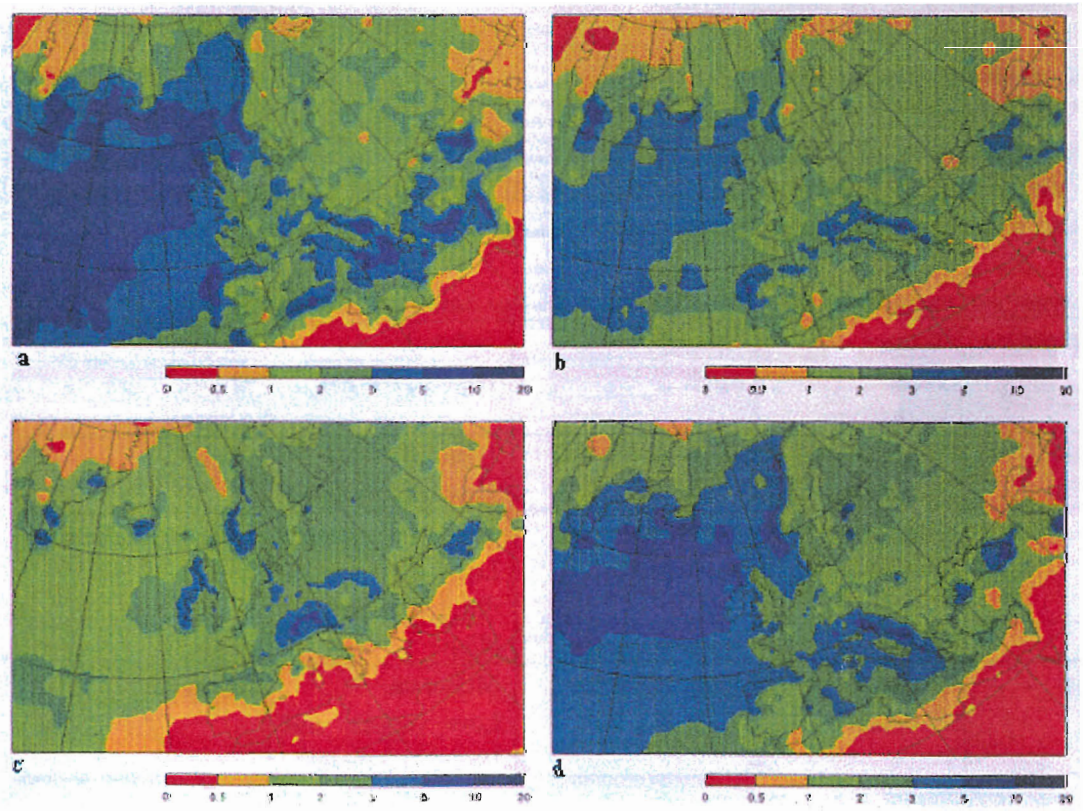

Figure 2.3 Mean precipitation (in mm/day) for winter (e), spring (f), summer (g) and autumn (h). Terrestrial data time period is 1920-1980, oceanic ship data: 1950-1979 (Legates and Willmott, 1990b).

Oceanic climate and altered oceanic climate (area 1 and 2 in fig 2.1) have much precipitation in all seasons, with peaks for North-West Spain, the west shoars of Ireland, the UK and Norway. There are small areas at the leeward side of the mountains which receive few precipitation, but the effect on meso-scale research in this report is negligible. There is no shortage of rain in general and it is distributed quite homogenoues at most times. The continental climate (area 3) zone receives less precipitation in winter than in summer, except for the mountain areas. It's behaviour is more convective and with more droughts intervals than the Oceanic types (apart from the showers above warm seawater in autumn).
The sub-arctic climate areas (area 5) have few precipitation in winter and spring (especially Sweden), due to the cold (and dry) air masses which generate often static high pressure areas in that region. In summer and autumn there is considerable more rain, due to the northern position of the polar jetstream.
The Mediterranean area (area 3) receives huge amounts of precipitation in autumn and winter, when the polar jetstream is present. The unstable air above the relatively warm seawater picks up a lot of water vapour then. In spring, the influence of the subtropical desert area with descending stable air is more noticeable, and precipitation events are less frequent. In summer, substantial precipitation is at northern regions only. The polar jetstream is located at high latitudes then, keeping away the rain carrying low pressure systems and frontal areas. Only scattered showers occur. It is remarkable anyway that total annual precipitation is exceeding averaged European precipitation. Only South-East Spain is suffering more systematical drougths.

2.2 Implications for soil moisture

The knowledge of temperature, precipitation, and duration of solar radiation provides some qualitative information about the seasonal availability of soil moisture for evapotranspiration and runoff generating. This will be discussed for the areas, according to the modified Köppen climate classification (see Figure 2.1). A very rough indication for the change in soil moisture ($\Delta\theta$), disregarding other factors like soil properties and interception, is the balance between precipitation (P) and actual evapotranspiration (E_a):

$$\Delta\theta \approx P - E_a \approx \text{net advection of water} \qquad [2.1]$$

When P- E_a is positive, the soil moisture will increase if the soil is not saturated. In saturated conditions, the advection term is roughly equal to the surface water runoff. When P- E_a is negative, soil moisture will decrease until no water can be extracted from the soil anymore.

Table 2.1 Seasonal soil moisture content for climate types areas based on climatology only

climate ↓ \ season →	Winter	Spring	Summer	Autumn
Oceanic	High/ excessive	High	High/moderate	High/ Excessive
Altered oceanic	High/ Excessive	High/moderate	High/moderate, Low (dry periods)	High
Continental	High/ moderate	High/excessive, moderate	High to moderate, Low (at longer drought periods)	High to moderate
Sub-Arctic	High	High/excessive	High	High
Mediterranean	High/ Excessive	High/moderate	Moderate, Low (upper soil layers in general)	Moderate

Oceanic climate

The annual amplitude of both the mean precipitation and temperature is small. Because of the constant supply of water into the soil, soil moisture content is always high, apart from short term dry periods in summer when E_a may exceed precipitation. In winter, the shorter day length reduces E_a to a minimum, but not to zero. The high average windspeed at the coast however boosts up the E_a somewhat. Excessive soil water may result in increased runoff (e.g. deep runoff and surface runoff) or even floodings.

Altered oceanic climate

The annual temperature amplitude is higher (> 15 °C), while the precipitation regime is simular to the oceanic climate. The soil moisture content in winter is always high, and E_a is reduced further in comparison to the oceanic climate because of the lower temperature and windspeed. Runoff is enhanced by this circumstances. In summer however, precipitation is distributed more variable and longer dry periods occur. Combined with high temperatures, this may result in considerable decrease of soil moisture content, when the evaporative demand by growing vegetation is highest. But in general, soil moisture content is sufficient high for evapotranspiration during the year.

Continental climate

The temperature amplitude increases further and precipitation is more variable, also in the winter season. Now, storage of snow is getting important in winter which causes high soil moisture levels in spring when snow melting occurs. The daylight conditions are the same for the climate type areas 1, 2 and 4 (fig 2.1), and the solar radiation is thus roughly constant. In summer, frequency of dry periods increases, in comparison to the oceanic climates.

Sub-arctic climate

The difference in temperature between winter and summer is large (> 20 °C). But now, the amplitude in daylight duration (thus net radiation) and the low winter temperatures are involved. In January mean temperature drops below freezing point at which only sublimation of ice may occur. Moreover, the net radiation is very low in winter which actually reduces E_a to zero. In spring, large quantities of melting water are feeding the soil reservoir, that is very small due to permafrost in most soils. This keeps the soil moisture content high, although precipitation is low. In summer, precipitation increases and low average temperatures prohibit large E_a. Soil moisture is thus high all over the year, just like the oceanic climate areas.

Mediterranean climate

In contrary to the sub-arctic climate, there is relatively less variation in duration of daylight, so potential evapotranspiration is high during the whole year. The relatively high mean temperature in winter (> 10 °C) causes substantial E_a, which is exceeded by the rainfall. Soil moisture reservoir fills up and some places are subject to excessive runoff then. During spring and summer, E_p increases, but E_a drops to a minimum due to scarcity of rain. Soil moisture decreases sharply, especially in the upper soil layers. Some areas, like Southern Portugal (pers. com. Bosveld, 2000), have increased E_a caused by extensive irrigation! In autumn, soil moisture content increases again.

Table 2.1 shows an overview of the implications for P- E_a to θ for all seasons and climate types in Europe. The qualitative classification will be coupled to some soil hydraulic properties used in the next chapters. The classification "excessive" are refering to maximum values of θ (θ_s). "High" refers to $\theta_{\text{field capacity}}$ (θ_{cap}), at which plant roots still do not suffer from drought stress and maximum evapotransipration

occurs. "Low" refers to $\theta_{\text{permanent wilting point}}$ (θ_{pwp}), when the plant roots are not able anymore to extract water and to transpire it. Soil moisture at "Moderate" lies between (θ_{cap}) and (θ_{pwp}) and E_a is limited then.

Chapter 3 Model description

The core task of a land surface parameterization scheme (TESSEL in this research) is to take care of the water and energy fluxes between a soil reservoir with vegetation coverage and the boundary layer of the atmosphere. Temporal and spatial boundary conditions for the atmospheric or climate model (RACMO) are provided by the land surface parameterization. Therefore, it is very important to parameterize structure of the soil and its physics properly.
The structure of soil particles determines the conductivity for water transport and the vertical distribution of (volumetric) soil moisture content (θ). This distribution affects the evapotranspiration that connects the surface water- and energy budgets.
Relevant information about the composition of soils, the relation pressure head-water content, and the hydraulic parameters for the Richards' equation are discussed in § 3.1.
The structure of TESSEL is subject of § 3.2. Apart from that, the paragraph will focus on the conventional representation of soil hydraulic properties by Clapp and Hornberger (CH) parameterization and the implementation of the Mualem-van Genuchten (MVG) parameterization, based on the HYPRES (Hydraulic Properties of European Soils) soil map (Alterra, 2000). Finally, the basic configuration for Europe of the host atmospheric model RACMO will be discussed briefly in § 3.3.

3.1 Soil hydraulic properties in general

Soils are very complex in their composition and quite variable in their occurrence and properties. Despite this intricate nature, soils can be handled and studied systematically. Figure 3.1 shows the phases in soils: solid (a), liquid (b) and gas (c). The solid phase, which consists of mineral and organic matter, forms the matrix or 'skeleton' of the soil. This matrix is not always rigid, as the word 'solid' suggests. Certain soils swell and shrink, i.e. the solid phase particles move with respect to one another. This complex effect is not taken into account in long-term weather and climate models. More important is the volume of the spaces between the solid particles, called soil pores. They form a continuous space throughout the soil and are determined by the shape, size and arrangements of the solid particles (Koorevaar, 1993).

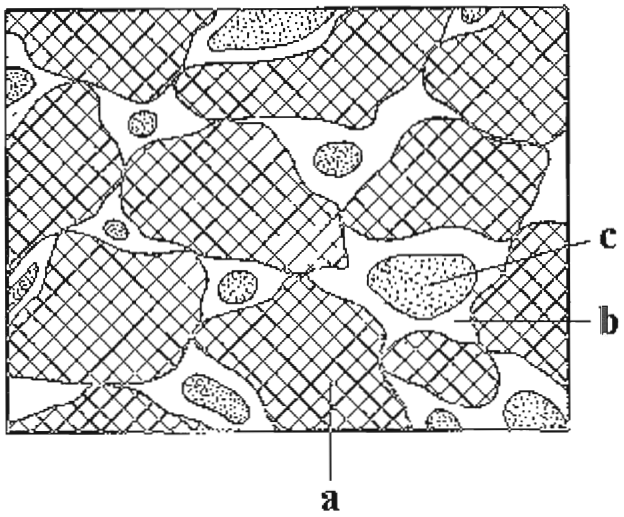

Figure 3.1 Composition of soil particles

Soil-texture classification

In many soils, the soil particles may vary widely in size, shape and composition. The particle-size distribution is called **texture.** These soil-textures vary little in time and can be used to classify soils. Certain ranges of particle-sizes are grouped into categories, defined by the FAO (1990):

Sand	2000-50 μm
Silt	50-2 μm
Clay	< 2 μm

A soil can now be classified, based on the weight distribution of these categories.

Volumetric water content and pressure head

To calculate how much water is stored in a soil layer, the porosity (ϕ) is introduced which is defined as:

ϕ = Total volume of pores / total volume of soil (m^3/m^3) [3.1]

This defines directly the maximum amount of water that can be stored per volume soil, the maximum or saturated volumetric soil moisture content (θ_s). The volumetric soil moisture content (θ) is thus expressed as:

θ = Volume of water / total volume of soil (m^3/m^3) [3.2]

The next important parameter for soil physics is the pressure that soil moisture exerts in the soil. This pressure is expressed in energy per weight (m), the pressure head h. The background concepts of h, deduced from the potential theory, are explained in Appendix A.1.

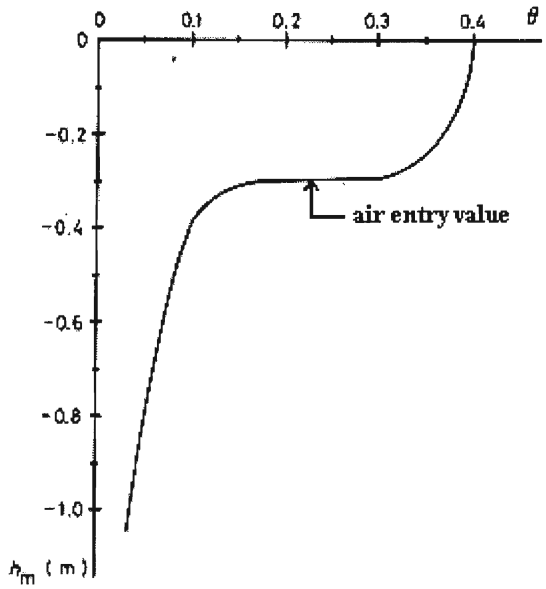

Figure 3.2 Example water retention curve

The relation between the volumetric soil moisture content (θ) and the pressure head (h) is characteristic for different soil types. It is called the *water retention curve*. Figure 3.2 shows one for a coarse sandy soil. In this example, θ decreases almost instantly from 0.3 to 0.1 $m^3\ m^{-3}$ at h = -0.3 m. At that point, the large pores of the soil are emptied. When pressure head decreases further, the decrease of θ goes slower.

In soils that contain finer textures, a more gradual release of water is found when the pressure (or matrix) head is decreased from $h = 0$ to $h \approx -10^4$ m. It is difficult to plot the whole water retention curve in one graph, unless h is plotted on a logarithmic scale. For that purpose, the pF expression is convenient:

$$pF = {}^{10}\log(-h) \qquad \text{(h expressed in cm)} \qquad [3.3]$$

Different values for θ and h, which have implication for the evapotranspiration and drainage, are shown in Table 3.1. These values are very important for the analysis of the water balance in chapter 4, especially for studying changes in the water balance terms among different soils.
The meaning of θ_s, θ_{cap} and θ_{pwp} has already been partly discussed in § 2.2. θ_s is assumed to be equal to ϕ; but at field, θ_s is ca. 0.85-0.95 ϕ. The qualitative indication in the most right column of Table 3.1 refers to Table 2.1, where the relation between climate types in Europe and soil moisture is summarized. When excessive percolation has stopped after few days, when the soil was saturated by heavy rain or irrigation, the specific value of θ is called field capacity (θ_{cap}). When pF > 4.2, plant roots cannot extract water anymore. Soil moisture at that threshold is therefore called permanent wilting point (θ_{pwp}). θ_r is the amount of water that can only be extracted from the soil particles at extreme low pressures and high temperatures. During normal weather conditions, θ_r will stay around the soil particles (due to direct adhesion of water molecules to solid surfaces by London-van der Waals forces) and doesn't contribute to the soil water balance. For plants, the range of θ between θ_{cap} and θ_{pwp}, also called *the dynamic soil moisture range,* affects the transpiration. This available soil water can be derived in the water retention curve by looking at the values of θ between pF = 2 and 4.2. Water held at high values of h (pF < 2) is not available for plants because it percolates fast through the root zone to the subsoil. Shortage of oxygen for plant roots near θ_s is disregarded in this research. Values of θ between θ_s and θ_{cap} have an important effect on the runoff (drainage/deep runoff + surface runoff) and bare soil evaporation.

Table 3.1 Important values of θ

		θ ($m^3\ m^{-3}$) (depends on soil-texture)	**Pressure head (m) and pF (-)**	**Indication** (in Table 2.1)
Saturation	θ_s	ranging from ca. 0.4 (sand) to 0.9 (young peat) $m^3\ m^{-3}$	$h = 0$ m , pF = - ∞	excessive
Field capacity	θ_{cap}	ca. 0.1 (sand) to 0.6 (peat) $m^3\ m^{-3}$	h = -1 m , pF = 2	high
Permanent wilting point	θ_{pwp}	ca. 0.03 to 0.4 $m^3\ m^{-3}$	h = -160 m , pF= 4.2	low
Residual water	θ_r	ca. 0.01 $m^3\ m^{-3}$	h = << -160 m , pF = ca. 6	very low

To quantify soil water transport, knowledge of the relation between θ, h and the soil properties that influence the water fluxes is required.

General soil moisture relation: the Richards equation

The general equation for 1D-soil water flow, based on the mass continuity equations and Darcy's law, is the Richards' equation (see Appendix A.2 for its derivation):

$$\frac{\partial \theta}{\partial t} = -\frac{\partial}{\partial s}\left(D(\theta)\frac{\partial \theta}{\partial s}\right) + \frac{\partial}{\partial s}\left(k(\theta)\frac{\partial z}{\partial s}\right) \qquad [3.4]$$

This is a non-linear differential equation of the second order. The equation is solved for one dimension (direction 's'). The coordinate directed downwards (z) is the same as 's' for TESSEL. The mathematical description of a particular flow problem needs boundary conditions and also initial conditions, when time-variant problems are involved.
For each soil type, the soil hydraulic conductivity or diffusivity are specified as functions of water content, but are actually based on the pressure (or matrix potential) gradients. In the current control version of TESSEL, relations of Clapp and Hornberger (1978) are used. The modified TESSEL uses the Mualem-van Genuchten relations for k and D (§3.2.3).

3.2 Setup ECMWF 1995 Scheme and TESSEL version

This paragraph consists of three parts: the first part shows the general setup of TESSEL and discusses the relevant soil hydraulic properties of the ECMWF scheme (Viterbo and Beljaars, 1995) in more detail. The connection between the surface energy and water balance will be analyzed briefly. In the second part, special attention is paid to the variable HYPRES soil map for Europe. The CH and MVG relations are subject of the third section.

3.2.1 Structure of TESSEL and soil hydraulic aspects

A full description of all features of TESSEL would be too extensive for this report. The official paper is in preparation (Viterbo et al., 2000). But the basic features are derived from the current operational ECMWF LSP scheme (Viterbo and Beljaars, 1995). Discussing figure 3.3 will highlight the relevant subjects.

There are four basic soil layers (s_1 ..s_4). The differential equations for heat and water transport are solved for each layer. The thickness of the layers is based on their representations of the different time scales. The upper layer s_1 has to deal with diurnal fluctuations of e.g. solar radiation and precipitation, while layer s_4 'remembers' seasonal processes. When harmonic waves are absorbed by the upper layer, their amplitude decreases, the wavelength increases and there is phase shift (delay) in deeper layers (Warrilow et al., 1986).
Important for the water balance, is the interception reservoir (M), which represents evaporation from a thin layer of intercepted water on vegetation and soil. Introducing a (virtual) skin layer, which represents vegetation and litter on bare soil, improves the parameterization of the surface heat balance. It has no heat capacity, isolates the radiative heating from the soil layers below, and interacts immediately with atmospheric forcing. The top boundary conditions for the soil-system are the net heat flux for the surface energy balance and the infiltration (precipitation minus surface runoff and evaporation from the interception layer) for the water balance. The bottom boundary conditions for the water balance is the deep drainage from the bottom layer s_4 and the evapotranspiration.

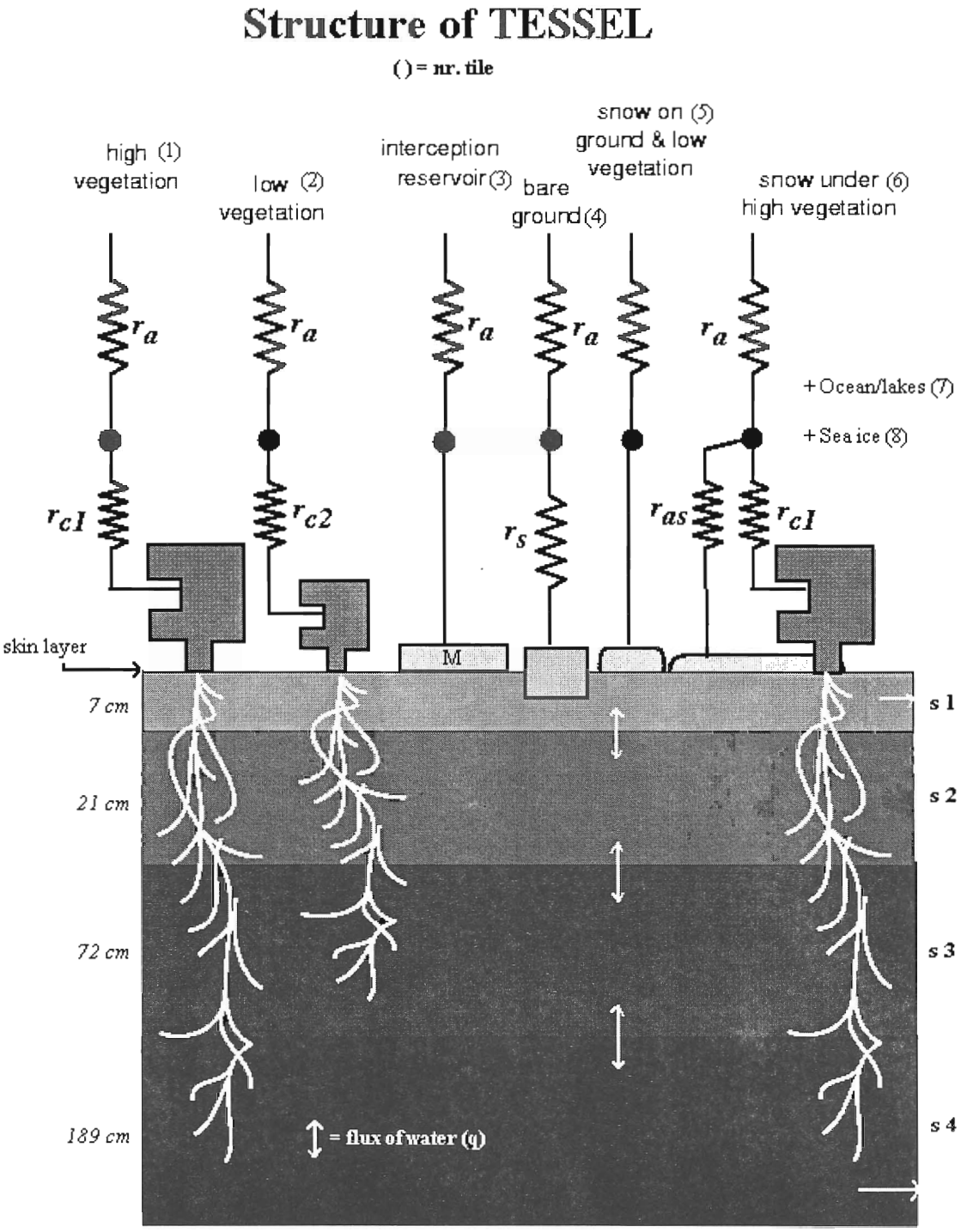

Figure 3.3 General setup TESSEL

Tiles and vegetation

As already indicated in chapter 1, in TESSEL each grid box is divided in fractions or tiles. These tiles produce heat and water fluxes separately. These fluxes are then area-averaged to yield the bulk fluxes for the atmosphere model (RACMO in this case). For meso-scale grids, the underlying assumption is that all tile-fluxes have been 'mixed' completely. The tiles can be classified into bare soil, vegetation, snow/ice and water. A description of the parameters can be found in Appendix B.

The link between the surface energy and water balance

Energy balance:

$$H + L\underline{E} + G = Q^* \qquad (\text{W m}^{-2}) \qquad [3.5]$$

Water balance for soil system:

$$P = \underline{E} + R + \Delta W_s + \Delta W_{sn} \qquad (\text{mm or m}^3\,\text{m}^{-2}) \qquad [3.6]$$

Where,

H = Sensible heat flux, that heats up or cools down the air
LE = Latent heat flux, in which L is the energy needed for evaporating water and snow
G = Soil heat flux
Q^* = Net radiation flux (incoming minus outcoming short-wave and long-wave radiation)

P = Total precipitation in gridbox
E = Evapotranspiration (sum of evaporation from bare soil, water and vegetation)
R = Total runoff (sum of surface runoff and deep runoff/drainage)
ΔW_s = Storage change of liquid water in the total soil system (sum of 4 layers)
ΔW_{sn} = Storage change of solid water in the total soil system (snow/ice and frozen soil moisture). The subscript c stands for "cryosphere".

The total evaporation or evapotranspiration (E) at the land surface is strongly entangled within the energy and water balance and will be discussed in more detail. The role of the evapotranspiration in the water budget is evident and for the energy budget it influences the partitioning of solar net radiation used for heating the air (sensible heat flux) and to evaporate water (latent heat flux). The other terms of the water balance are subject of chapter 4.

For evapotranspiration, several resistances are important (see also Appendix B):
1. The aerodynamic resistance (r_a), expressing the aerodynamic exchange between the surface at reference height (z_{0h}) and the well-mixed boundary layer.
2. The surface resistances that comprise (a) the canopy resistance (r_c, regulating the transfer and evaporating water through the stomata) and (b) the bare ground resistance (r_s, regulating the bare soil evaporation)

The canopy resistance (r_c) in TESSEL, which acts as a kind of valve, affects the transpiration. It is a function of:

1. Downward short-wave radiation (Q_s)
2. Leaf Area Index (LAI)
3. Atmospheric water vapour deficit (D_a)
4. Minimal stomatal resistance ($r_{s,min}$)
5. **Soil moisture content (θ)**

Expressed in formula:
$$r_c = \frac{r_{s,\min}}{LAI} f(Q_s) f(D_a) f(\theta) \qquad [3.7]$$

Only $f(\theta)^{-1}$ will be discussed, because it concerns the soil moisture content and its vertical distribution:

$$f(\theta)^{-1} = \frac{\overline{\theta} - \theta_{pwp}}{\theta_{cap} - \theta_{pwp}} \quad \text{if} \quad \theta_{pwp} \le \overline{\theta} < \theta_{cap}, \quad 0 \text{ if } \quad \overline{\theta} < \theta_{pwp}, \quad 1 \quad \text{if} \quad \overline{\theta} \ge \theta_{cap} \qquad [3.8]$$

The averaged value of θ (= $\overline{\theta}$), is the weighted mean of θ_l, the available *liquid* part of the soil moisture, per soil layer:

$$\overline{\theta} = \sum_{s=1}^{4} V_s \theta_l \qquad [3.9]$$

The percentage of the total root density (V) in each soil layer (s) is thus a weight factor for $\overline{\theta}$ and the stress for plant roots to extract water from the total soil system.
The canopy resistance is thereby (linear) proportional to the relative θ in the dynamic moisture range.

3.2.2 The variable HYPRES soil map

The original soil map of Europe consists of soil mapping units with characteristics of the upper and bottom soil texture. Recently, this information had been put in the HYPRES database (Wösten et al., 1999). After interpolation to RACMO gridscale, the dominant soil-texture from the HYPRES database has been assigned to each grid point. The textural composition of each soil is presented in Table 3.2 and visualised in figure 3.4. The 'histosols' are not based on soil particle size distribution, but on the ratio of organic carbon and mineral matter. The composition of a soil can be found by drawing a line parallel to the sand axis which shows the clay percentage. The line parallel to the clay axis marks the silt percentage and the rest is sand. A sandy soil for example may consist of 90 % sand, 8 % silt and 2 % clay, and the texture triangle defines the borders of the classes. This soil is classified as 'coarse' (C)

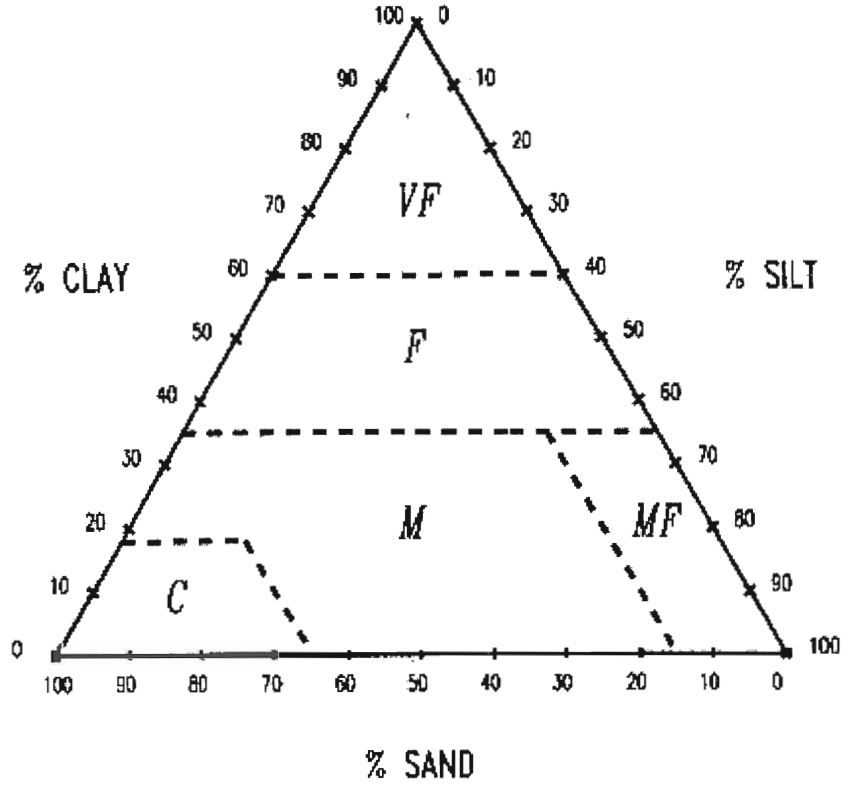

Figure 3.4 Texture triangle, according to European Union soil map .

Table 3.2 Standard FAO criteria for soil texture classes

Coarse	clay < 18 % and sand > 65 %
Medium	18 % < clay < 35 % and sand > 15 % OR clay <18 % and 15 % < sand < 65 %
Medium-fine	clay <35 % and sand < 15 %
Fine	35 % < clay < 60 %
Very Fine	60 % < clay
Histosol	organic carbon >12 % if clay = 0 % OR organic carbon >18 % if clay> 60 %

Fitting of the Mualem-van Genuchten curves by determining the MVG parameters was based on measured soil properties from each texture group. Per texture group several curves were fitted, one for each soil sample. The final MVG curve is the result of averaging those single curves: the class pedotransfer function (Wösten et al., 1998). In the HYPRES database there is a division between top soils and sub soils. In TESSEL, only the MVG parameters for the top soils are used, because there is no vertical distribution of texture-classes within each gridbox.

3.2.3 Clapp and Hornberger versus Mualem-van Genuchten parameterization

The first modification in this study was the implementation of a variable field soil grid in TESSEL. The second modification comprises the introduction of the Mualem-van Genuchten parameterization, which usually represents the water transport more realistically than Clapp and Hornberger, especially near saturation.

The functions for h, k and D, based on the work of Clapp and Hornberger (1978) are:

$$h(\theta) = h_{sat}\left(\frac{\theta}{\theta_{sat}}\right)^{-b} \quad , \quad k(\theta) = k_{sat}\left(\frac{\theta}{\theta_{sat}}\right)^{2b+3} \quad \text{and} \quad D(\theta) = \frac{bk_{sat}(-h_{sat})}{\theta_{sat}}\left(\frac{\theta}{\theta_{sat}}\right)^{b+2} \qquad [3.10]$$

The saturated pressure head is given by h_s, and b is the Clapp and Hornberger coefficient. These functions generate hyperbolic curves, for which the shape is determined by the exponent b.

The functions for h, k and D, based on the work of Mualem-van Genuchten (1980) are:

$$h(\tilde{\theta}) = \frac{\left[\tilde{\theta}^{-1/m} - 1\right]^{1/n}}{\alpha}, \quad k(\tilde{\theta}) = k_{sat}\tilde{\theta}^{l}\left[1 - \left(1 - \tilde{\theta}^{1/m}\right)^{m}\right]^{2} \text{ and}$$

$$D(\tilde{\theta}) = k(\tilde{\theta})\left(\frac{1-m}{\alpha m(\tilde{\theta}_{sat} - \tilde{\theta}_{r})}\right)\left(1 - \tilde{\theta}^{1/m}\right)\tilde{\theta}^{-1/m} \qquad [3.11]$$

Here, a few more parameters are involved than in the CH parameterization. For simplicity, the soil moisture ($\tilde{\theta}$) is written as (θ - θ_r) / (θ_s - θ_r). New are α, n and l which determine the shape of the curves (m = 1-1/n). The inverse of the air entry value (pressure head h at which all large soil pores are emptied) where $d\theta/dh$ has its maximum value, is indicated by α (cm^{-1}). The dimensionless parameters l and n determine the exact steepness and position of the typical S-shaped curves.

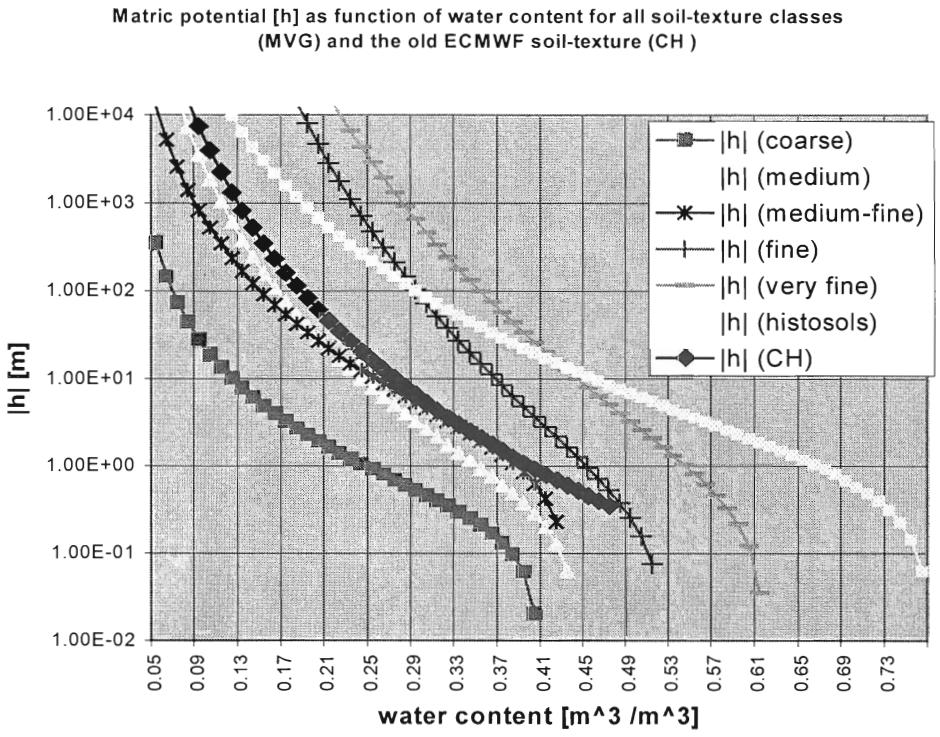

Figure 3.5 Retention curves for soils, based on CH and MVG parameterization

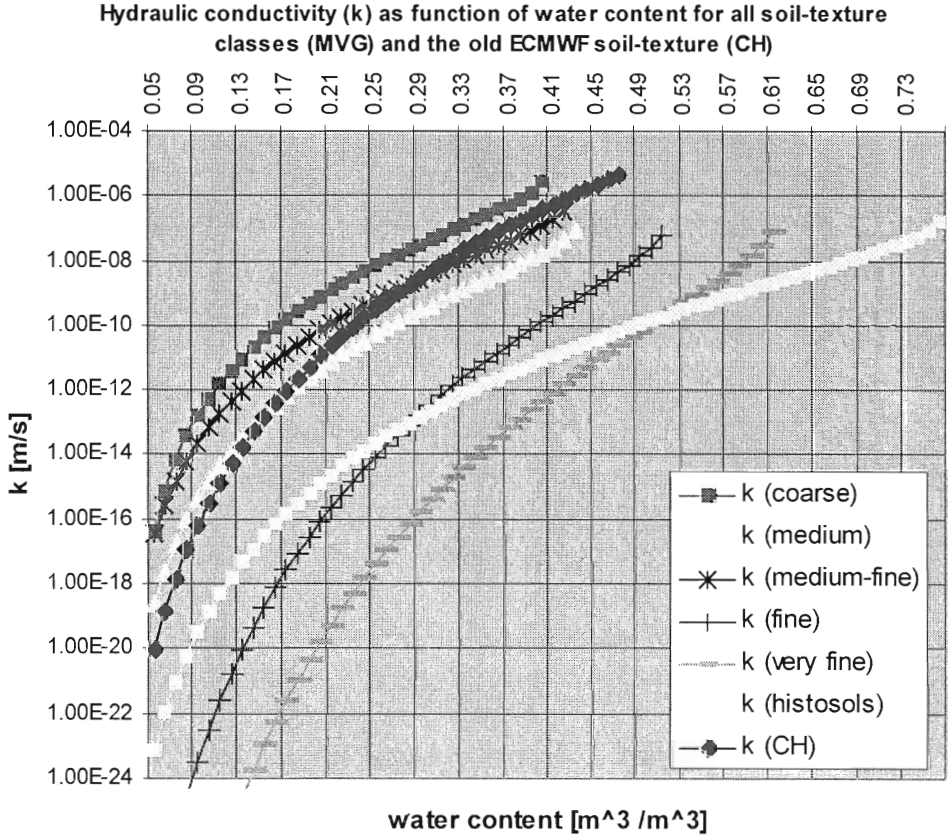

Figure 3.6 Hydraulic conductivity (k) for soils, based on CH and MVG parameterization

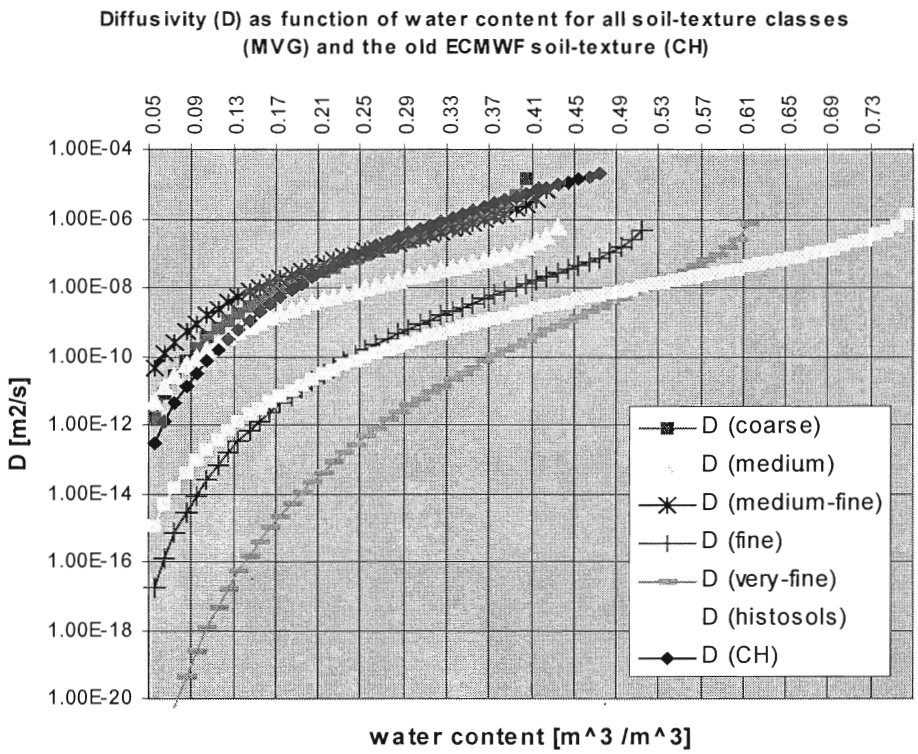

Figure 3.7 Diffusivity (D) for soils, based on CH and MVG parameterization

Table 3.3 a Parameters for mean soil derived by Cosby et al. (1984), based on Clapp and Hornberger parameterization (1978).

Soil texture	h_s (m)	θ_s ($m^3\ m^{-3}$)	θ_{cap} ($m^3\ m^{-3}$)	θ_{pwp} ($m^3\ m^{-3}$)	k_s ($m\ s^{-1}$)	b (-)
Comparable to '**Medium**'	-0.338	0.472	0.323	0.171	4.57E-06	6.04

Table 3.3 b Parameters for texture classes in HYPRES, based on Mualem-van Genuchten parameterization (1980).

Soil texture	α (cm^{-1})	n (-)	θ_s	θ_r	l (-)	θ_{cap}	θ_{pwp}	k_s ($m\ s^{-1}$)
Coarse	3.83	1.3774	0.403	0.025	1.2500	0.244	0.059	6.94 E-06
Medium	3.14	1.1804	0.439	0.01	-2.3421	0.347	0.150	1.16 E-06
Medium-fine	0.83	1.2539	0.43	0.01	-0.5884	0.383	0.131	2.63 E-06
Fine	3.67	1.1012	0.52	0.01	-1.9772	0.448	0.278	2.87 E-06
Very fine	2.65	1.1033	0.614	0.01	2.5000	0.541	0.333	1.74 E-06
Histosols	1.3	1.2039	0.766	0.01	0.4000	0.663	0.265	9.26E-07

Table 3.3 c Available water for transpiration (θ_{cap} minus θ_{pwp}) (in $m^3\ m^{-3}$)

Control (C&H)		Coarse	Medium	Medium-fine	Fine	Very fine	Histosols
0.15		0.19	0.2	0.25	0.17	0.21	0.40

Table 3.3 d Hydraulic conductivity k ($m\ s^{-1}$), and diffusivity D ($m^2\ s^{-1}$) at θ_{cap}

	C&H	Coarse	Medium	Medium-fine	Fine	Very fine	Histosols
k	1.50 E-08	0.54 E-08	0.24 E-08	6.55 E-08	0.15 E-08	0.09 E-08	0.69 E-08
D	93.6 E-08	7.56 E-08	5.05 E-08	156 E-08	4.11 E-08	2.26 E-08	8.90 E-08

Table 3.3 a and b summarize all coefficients for both the Clapp and Hornberger and Mualem-van Genuchten parameterizations. The difference between θ_{cap} and θ_{pwp} is the available water for transpiration, see Table 3.3 c. The values for k at θ_{cap} and θ_{pwp} are mentioned in Table 3.3 d.

The functions $h(\theta)$, $k(\theta)$ and $D(\theta)$ are plotted in figure 3.5 until 3.7 respectively. The retention curves in figure 3.5 show that θ_{coarse} is always lower than θ_{CH}, when the situation is regarded from differences in pressure heads between θ_{cap} and θ_{pwp}. Soil moisture for 'fine', 'very fine' and 'histosols' (θ_{fine}, $\theta_{very\ fine}$, $\theta_{histosols}$) always exceed θ_{CH}, while θ_{medium} and $\theta_{medium\text{-}fine}$ are almost equal to the Clapp and Hornberger soil moisture content. Recall that the dynamical moisture range lies between $|h| = 1$ (pF = 2) and $|h| = 159$ m (pF = 4.2), indicated by thick horizontal lines in the graph.

The plots for hydraulic conductivity as function of θ in Figure 3.6 reveal that most MVG soil-textures have lower k than the CH soil. Only k_{coarse} is higher than k_{CH}. Only at very wet conditions, comparison is possible between the soil textures "coarse", "medium", "medium-fine" and the CH soils, because their soil moisture at saturation (θ_s) is approximately the same. The values for k at ($\theta \leq \theta_{cap}$) are not relevant for runoff, because the matrix forces in the soil are stronger than gravitational force in that case. Table 3.3 d shows the values for k at field capacity, which gives more information about differences between the soil texture classes in distributing the precipitation over runoff and evapotranspiration at θ_{cap}. In general, the hydraulic conductivity is lower for the Mualem-van Genuchten than the Clapp and Hornberger parameterization.

The values for MVG diffusivity (D) are also lower than for CH (see figure 3.7). Remarkable is that medium-fine soils, in contrast to the other texture classes, have higher D than the CH soil at ($\theta \approx \theta_{cap}$), see Table 3.3 d. During drying conditions, moisture gradient is positive (downwards). The diffusivity term (D) in the flux density equation is negative (upwards) in that case which may represent capillary supply of water from wet soil layers at the bottom towards dry layers at the top. This medium-fine soil has thus optimal hydraulic properties for plants; during wet conditions ($\theta > \theta_{cap}$) there is fast drainage due to relative high k, which prevents shortage of oxygen for plant roots. During dryer conditions ($\theta < \theta_{cap}$), there is a re-distribution of soil water from wet to dry soil layers due to a relatively high D. When the soil is very wet ($\theta > \theta_{cap}$), D is not important because the influence of k is stronger then.

3.3 Main characteristics of hostmodel RACMO

TESSEL is hosted by RACMO (Regional Atmospheric Climate Model) (Christensen et al., 1996). RACMO is a tool for studying and developing parameterizations in large scale weather and climate models. Physical processes, based on the ECHAM4-GCM (Roeckner et al., 1996), are emphasized. The dynamics are deduced from HIRLAM (Gustafsson, 1993), an operational regional weather model used by KNMI. This paragraph gives some basic information about the resolution and the interpretation of land and sea. Discussion about the aspects of modelling the atmospheric boundary layer and dynamics is beyond the scope of this research.

Vertical structure

The vertical structure of RACMO consists of 19 model layers. The representation of the air pressure and related parameters is of a so-called *hybrid* kind. Next schematic formula illustrates this:

$$Pressure(i) \approx a(i) + b(i) * \text{pressure at surface level} \qquad [3.12]$$

This coordinate system interpolates between a terrain following coordinate near the surface (b) and a fixed pressure coordinate at higher altitudes (a).

Horizontal structure and model configuration

The horizontal resolution of the gridboxes is approximately 50 km. Figure 3.8 shows the model domain with gridboxes and land-sea distribution. For this research, RACMO is used in the climate mode without internal updates after the initialization. The initialisation values are interpolated from ECMWF-analysis and the lateral boundaries from the model domain, with 6 hours time interval. Numerical timestep is 5 minutes, and the output is generated per 6 hours. The output consists of:

- *prognostic variables* (like pressure, temperature, wind speed in 2 directions, specific humidity, cloud cover, soil moisture etc.).
- *post-processing data* derived from prognostic fields of the previous time period (6 hours ago). These data represent the fluxes of water and energy at the land surface, like precipitation, evapotranspiration, latent heat flux etc.

Relaxation occurs from the corners of the model domain to smoothen the influence of the boundary conditions at the edges. This ensures that the output of grids near the boundaries of the model domain is not affected too much.

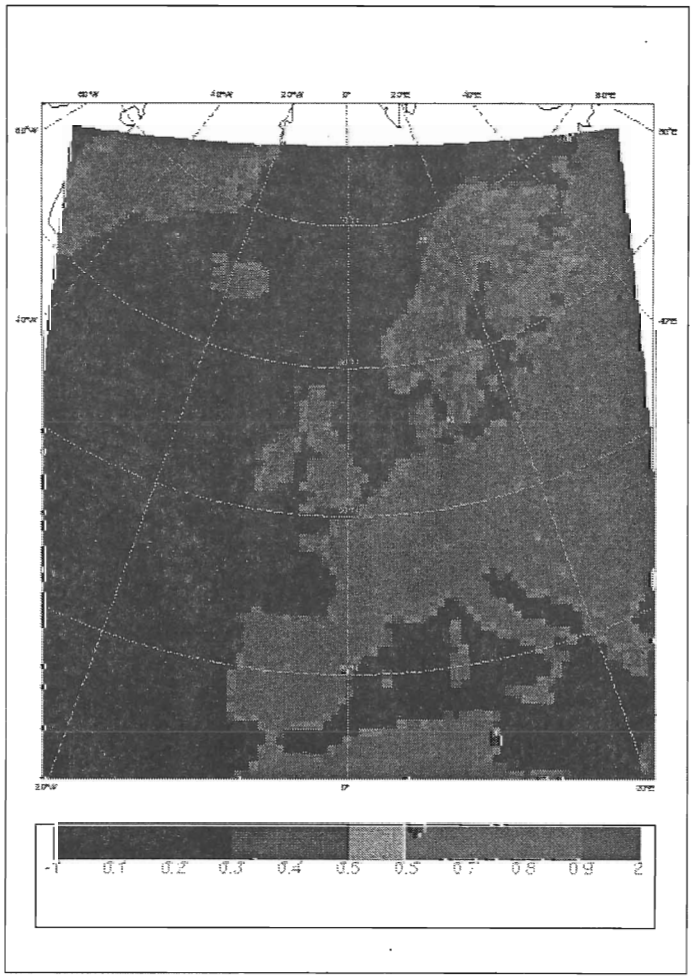

Figure 3.8 The land-sea distribution of the RACMO grid and its resolution

Chapter 4 Effect of variable soil texture field on the distribution of modelled surface water balance components at European scale

4.1 Introduction

Introducing the variable field soil map with Mualem-van Genuchten (MVG) parameterization, replacing the uniform Clapp and Hornberger (CH) field in TESSEL, is expected to cause shifts in the distribution of the terms in the water balance for most grid points. The reason for this is twofold. Firstly, the shape of the MVG-relations differs from the CH curves, also if the fittings of both types of curves are based on the same soil-texture. So, when MVG is applied uniformly, the hydraulic conductivity (k) as function of soil moisture content (θ) is different for both parameterizations. A comparison study of Cuenca et al. (1996) shows that evapotranspiration decreases then. Secondly, each gridpoint now has a specific soil texture and changed soil hydraulic properties. This second aspect is supposed to be dominant (enhancing evapotranspiration) for most part of Europe, as water availability increases for all MVG soil texture classes and hydraulic conductivity is smaller.

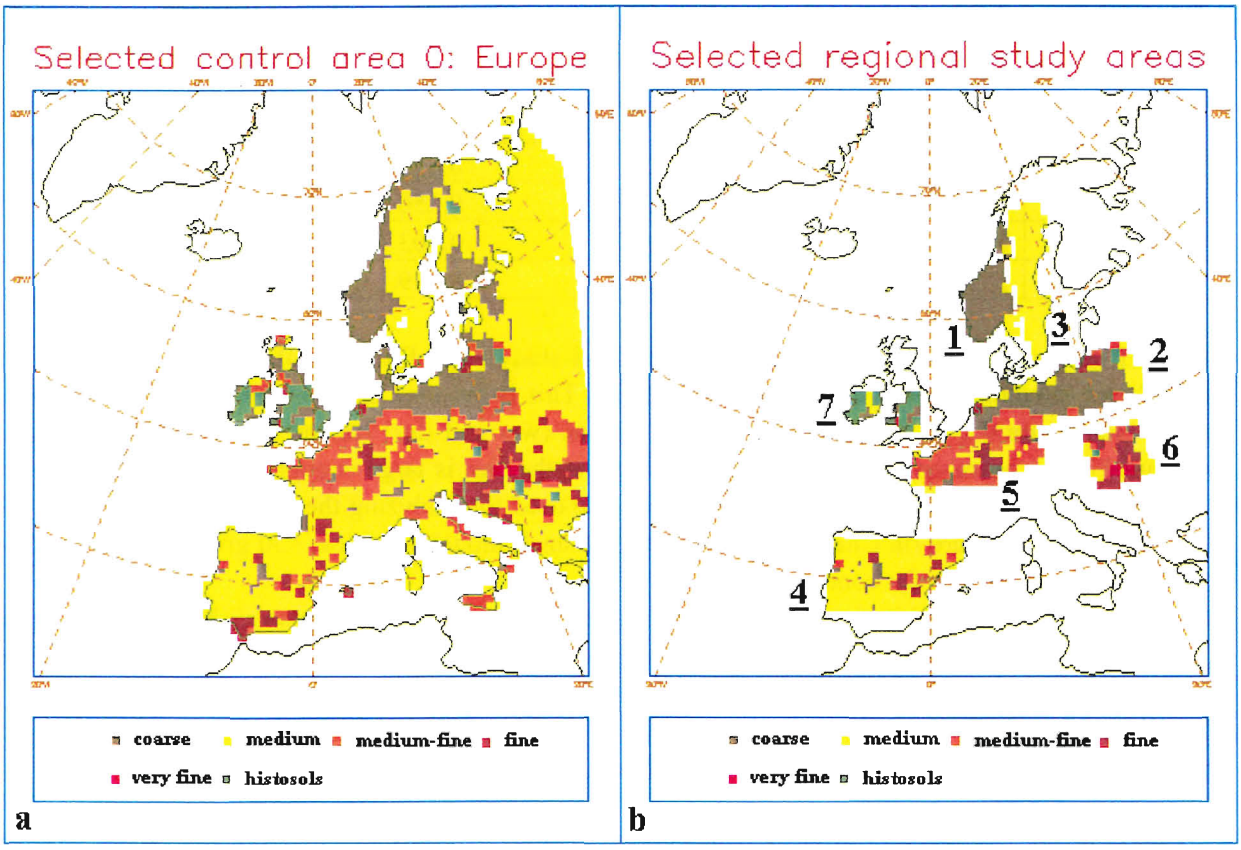

Figure 4.1 Distribution of soil texture classes for the control area (a) and regional study areas (b)

Regarding the gridpoints from Europa in total (control area) indicates the general effect of the variable soil map on the water balance. To analyze the water balance for each soil texture class, a selection of several regional study areas has been made. Details and criteria of this selection procedure are given in § 4.2. The discussion of the results will focus on the *time-series* of the accumulated water balance terms, averaged for the selected areas, in § 4.3. The *spatial distribution* of the terms, averaged per season is discussed in § 4.4. A major drawback of the model analysis is lack of observational verification. For one gridpoint however, the modelled runoff (the sum of drainage and surface runoff) could be compared to measured runoff in a polder at Cabauw in the Netherlands, discussed in § 4.5.

4.2 Setup analysis and description regional study areas in Europe

Figure 4.1 shows the HYPRES soil map database, interpolated to the RACMO grid for Europe.
The boundaries and the distribution of the soil texture classes of the control area (a) and the regional study areas (b) are marked.

The selection of the control area (area 0) comprises all land gridpoints of Europe, except Iceland. Particularly the water balance at the mainland of Europe is relevant for the aim of this research. Land gridpoints have a relative land area (seamask in RACMO) of more than 0.75. This excludes sea gridpoints from the analysis.

For the selected regional study areas (area 1 to 7), three general properties have been taken into account:
(a) soil texture class based on HYPRES soil map database
(b) size (nr. gridpoints) and ratio of gridpoints with specific soil texture class / total number of gridpoints
(c) climate type and its implication for the soil moisture regime (see Table 2.1)

Table 4.1 Properties of the selected regional study areas

Selected area	Texture class (a)	Size (b)	Ratio (b)	Climate type (c)
Area 1	Coarse	81	0.914	(Altered) Oceanic (wet)
Area 2	Coarse	171	0.696	Continental (dry)
Area 3	Medium	97	0.990	Sub-arctic (wet)
Area 4	Medium	158	0.835	Mediterranean (dry)
Area 5	Medium-Fine	120	0.550	Altered Oceanic
Area 6	Fine /Very Fine	66	0.303	Continental
Area 7	Histosol	36	0.639	Oceanic

Table 4.1 summarizes the properties for each regional study area. For each of the soil texture classes 'coarse' and 'medium', two areas have been selected. This is because they represent most gridpoints in Europe (see figure 4.1 a) and different climate regions (wet and dry) can be distinguished. The class 'Medium-Fine' is represented by only one selection, but the size is large enough to do a sound analysis. The size is important because the selected areas are also used for analyzing the relative humidity, specific humidity and temperature (in Chapter 5). Choosing too small model areas (ca. <50 gridpoints) may result in too few synops stations for comparison.
The problem of too few gridpoints arises for the classes 'Very Fine' and 'Histosols'. Moreover, the ratio of soil specific gridpoints for 'Very Fine' is rather low (0.303). So, the results for the soil texture classes 'coarse', 'medium' and 'medium-fine' are expected to be most reliable.

The model output to be analyzed for the water balance, see eq. [3.6], is:

- **Precipitation** (P), the sum of large scale (P_l) and convective (P_c) precipitation. For the time-series, only P is relevant. P_c is used for analysis of the assumed internal cycle of evapotranspiration and precipitation at the European mainland in summer.
- **Evapotranspiration** (E), sum of transpiration, interception evaporation and bare soil evaporation.
- **Total runoff** (R) and surface runoff (R_s). R_s will be used for the spatial distribution analysis.
- Change of water stored in snow (ΔW_{sn}). This term is component of the accumulated budget, but is not taken into account for analyzing differences between soil texture classes. For North Europe, this term is important in winter but is not relevant for this study.
- **Change of soil water storage** (ΔW_s). The storage (W_s) is the sum of the water content (θ) per soil layer (s) with thickness B. $W_s = \sum_{s=1}^{s=4} \theta_s B_s$.

4.3 Time series of soil hydrological budget terms

The time series for the water balance terms are very variable and sensitive to noise, which makes analysis of shifts between the CH and MVG output difficult for seasonal time-scales. Therefore, the elements of the water balance are plotted cumulative for the entire simulation period (March 1995 until July 1996), see figure 4.2.

4.3.1 Analysis of the control area: Europe

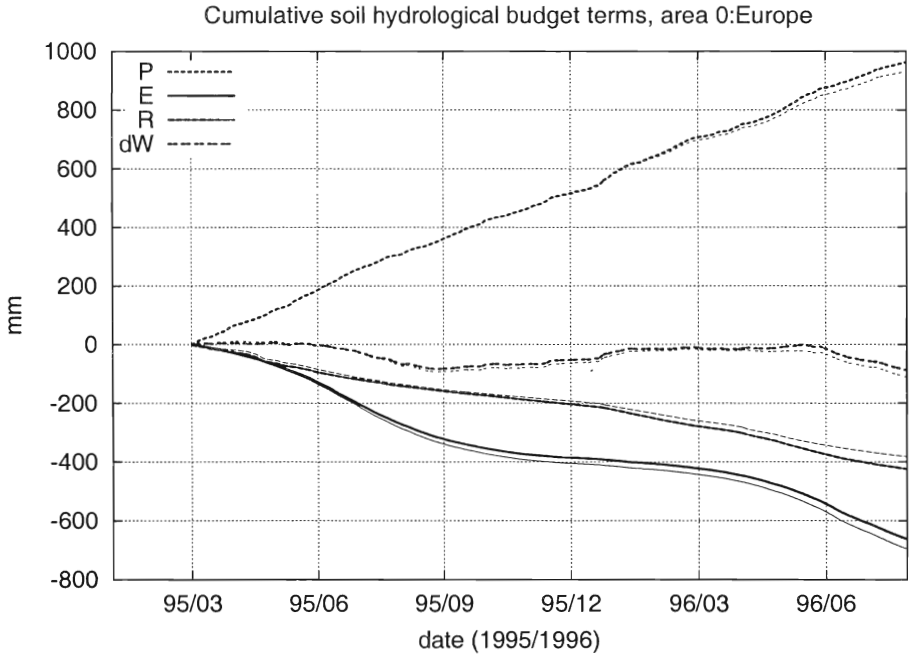

Fig 4.2 a

Figure 4.2 Cumulative plots of water balance terms for the control area (a) and the regional study areas for coarse (b and c), medium (d and e), medium-fine (f), fine/very fine (g) and the histosols (h). Shown are the results from the CH (thick lines) and MVG (thin lines) runs. (continued on next pages)

No systematical shifts between the CH and MVG precipitation (P) occur during 1995. From February 1996 on, MVG has lower values than CH, but this is probably due to some unreliable precipitation data at the eastern model border.

For the first control model (CH) run, initial soil moisture content appeared to be underestimated. After adjusting, ΔW_s (indicated as "dW"in figure 4.2) is zero again at spring 1996, like the modified model (MVG). Soil moisture reservoir is thus refilled in both runs. No significant shifts for ΔW_s occur between CH and MVG during the simulation period.

There is more evidence for a shift in R and E. Less runoff occurs at MVG than CH. This is caused by the lower hydraulic conductivity (k) for most soil textures in comparison to the CH soil type. Only the soil textures 'coarse' (if $\theta > \theta_{cap}$) and 'medium-fine' (if $\theta \approx \theta_{cap}$) have higher values of k. This means that the infiltrated water percolates slower through the soil layers, and more time is available for plant roots to transpire the soil water. Bare ground evaporation is enhanced too. Surface runoff (R_s) may increase as the frequency of upper soil layer saturation is larger (S_1, see figure 3.3). The contribution of R_s may compensate the decrease of R, especially in summer. The combination of lower k and increased total soil water storage (see table 3.2 c) for the MVG soils, thus probably enhances E. During the growing season, the deviation in E for CH and MVG is highest.

4.3.2 Analysis regional study areas

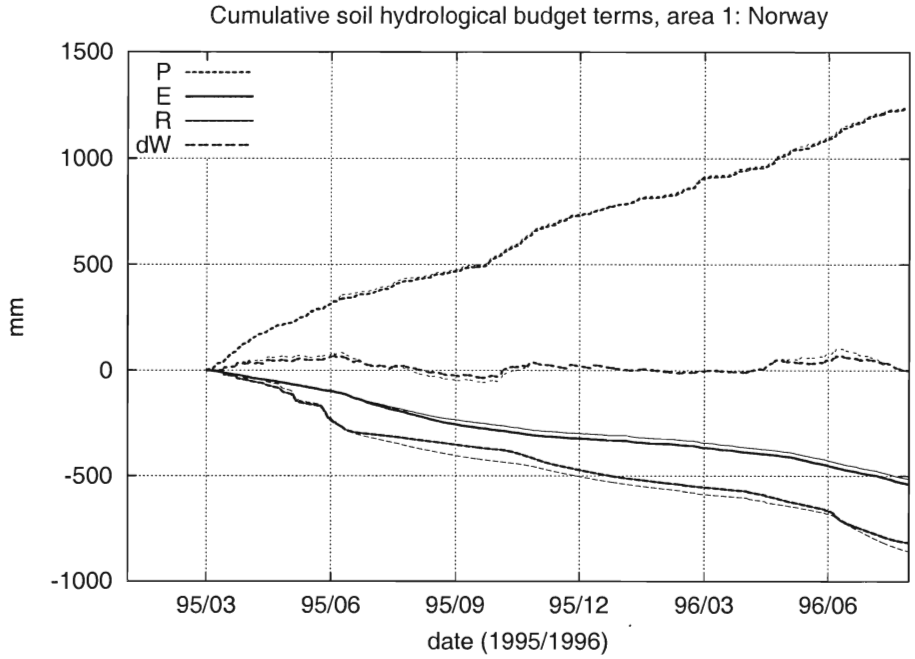

Figure 4.2 b

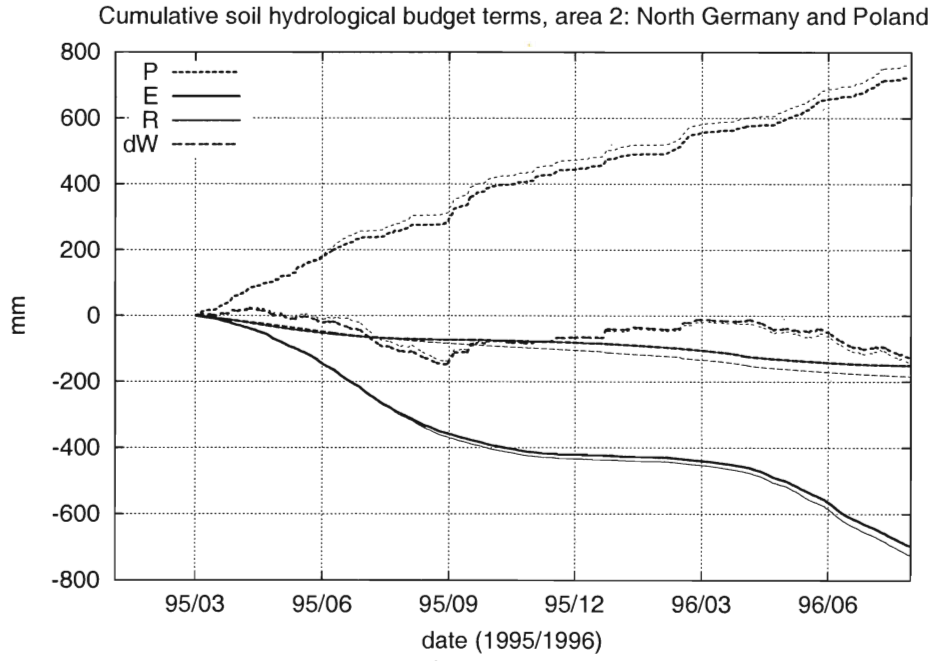

Figure 4.2 c

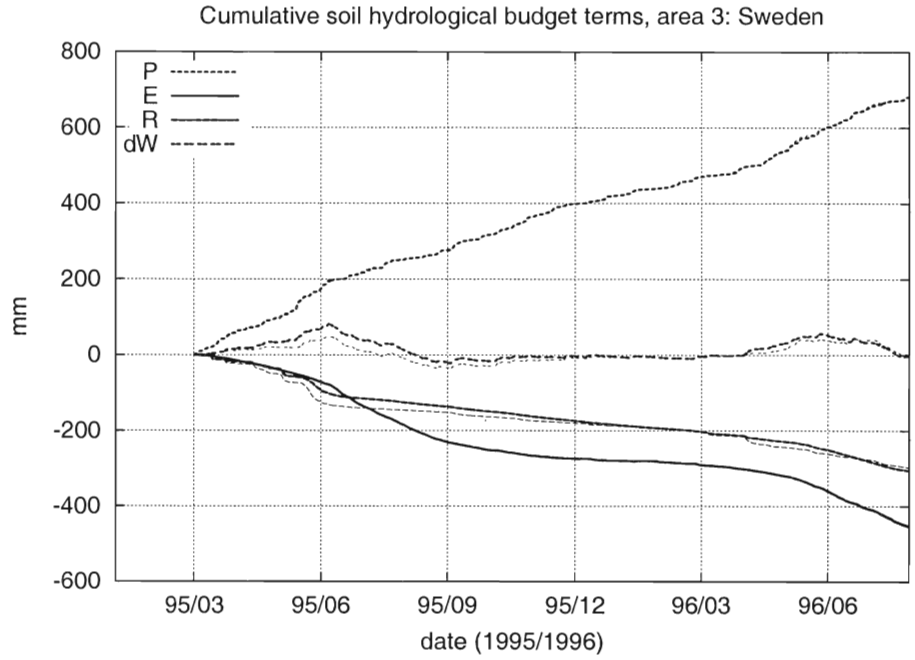

Figure 4.2 d

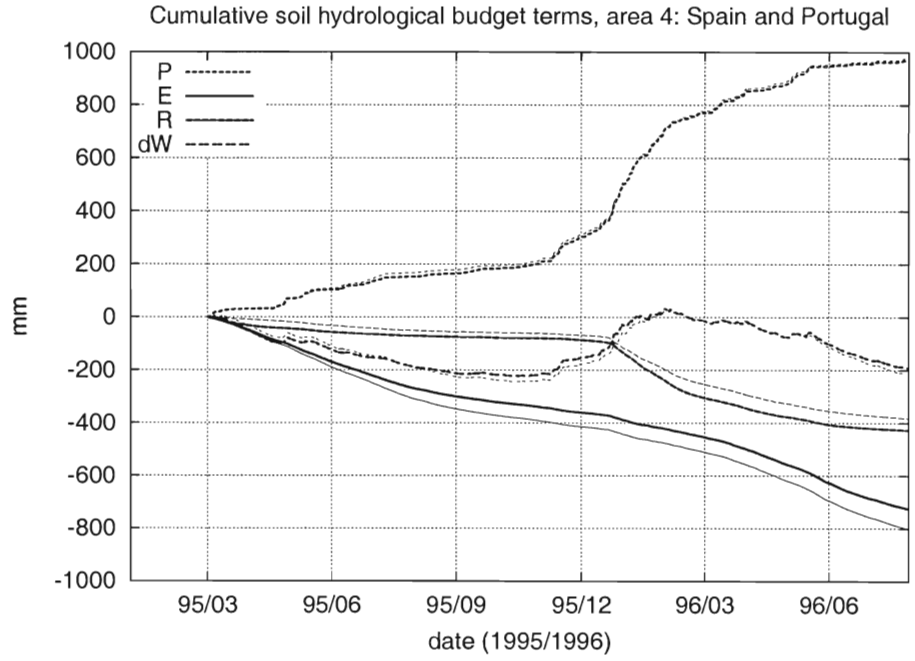

Figure 4.2 e

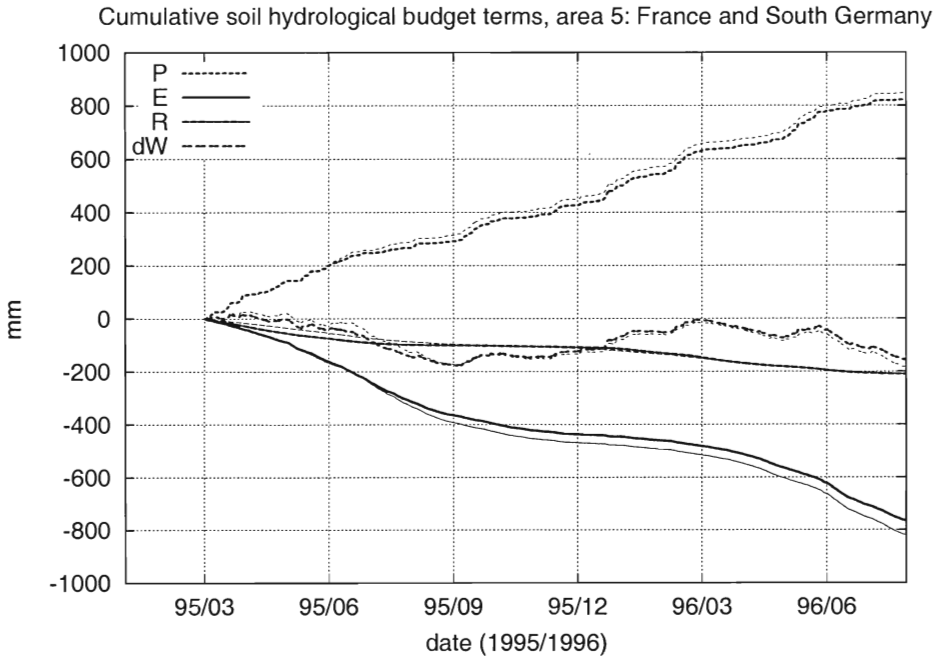

Figure 4.2 f

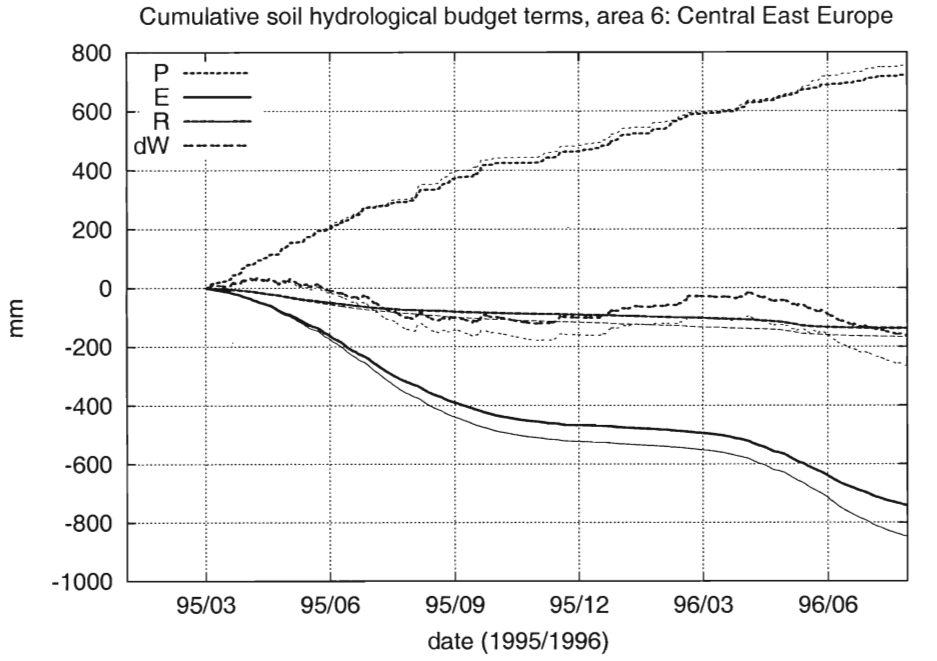

Figure 4.2 g

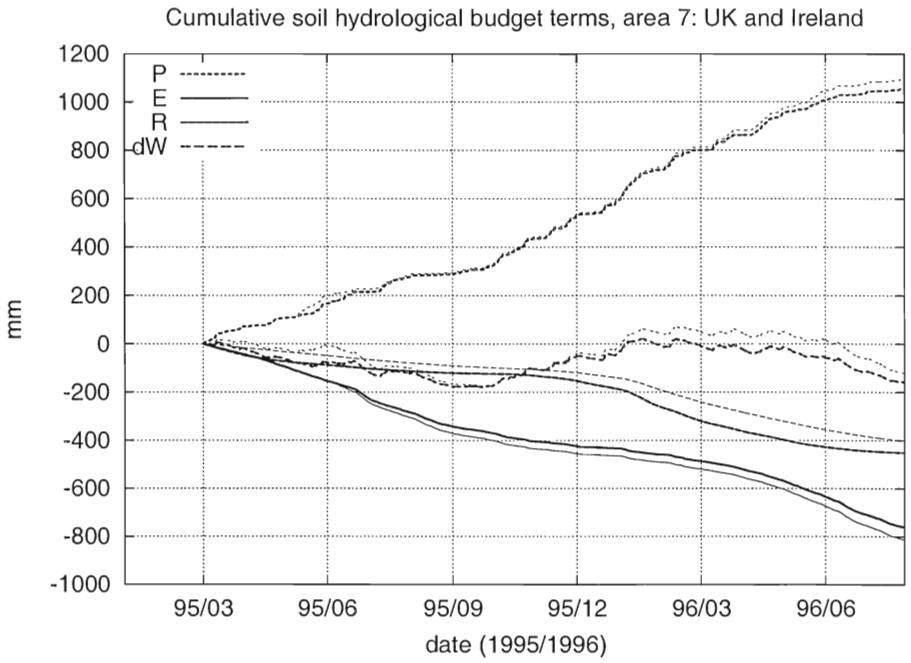

Figure 4.2 h

For the areas with **coarse** soil-texture (figure 4.2 b and c), precipitation deviates not systematically during the simulation period; an 'event' of increased P in June 1995 boosts up the cumulative budget for MVG for area 2, but lines are parallel during the rest of time.
There is evidence of increased runoff. ΔW_s between CH and MVG is negligible. For Norway (area 1), E_{MVG} is smaller (ca. 25 mm, ca 5 % of total E) than E_{CH}, but the difference is never more than a few millimeters. North Germany and Poland (area 2) however, face ca. 15 mm more (3 % of total E) E for the MVG run. Note that k_{coarse} for the *wet* ($\theta > \theta_{cap}$) area 1 is larger then k_{coarse} for the dryer area 2 ($\theta < \theta_{cap}$).
For the **medium** soil textures (figure 4.2 d and e), there is no significant effect on P and ΔW_s. For the wet and sub-arctic area Sweden (area 3), there is no effect on all budget terms, while in South Europe (area 4), E is significantly increased at the cost of R for the MVG simulation (> 50 mm). The effect of increased E is most distinct during the Mediterranean growing season in spring and summer; the period in which the bulk of transpiration occurs. After winter precipitation, the effect of decreased R is evident. This is caused by the lower k of medium soils in comparison to the CH soil-type, see figure 3.6.
The results of the **medium-fine** (figure 4.2 f and g) soils show that P has increased during summer, like area 2. In the area France-Germany (area 5), E is significantly larger for MVG. When all medium-fine gridpoints for Central Europe are included in the analysis (not shown), R is higher and ΔW_s is more negative. The higher k_{MVG} at field capacity conditions ($\theta \approx \theta_{cap}$) may explain this, while the higher diffusivity and available storage of water may cause the increased E.
The areas with soil texture "fine/very fine" and "histosol" have too few grid points for a sound analysis of the budget terms. The effect of local weather disturbs the interpretations of the results. The next statements are just indications about what may be going on.
Concerning soil-texture **fine/very fine**, R (up to 20 mm) and E (up to 50 mm) have increased, while the ΔW_s is more negative for MVG than CH (figure 4.2 g). The contribution of surface runoff to the total runoff is relatively high due to the low k.
For the **histosols** in the UK and Ireland, there are no large differences between MVG and CH parameterization (figure 4.2 h). E increases systematically during spring and summer. Here again, the increase of available soil water and the lower k play a dominant role.

4.4 Spatial and seasonal distribution of soil hydrological budget terms

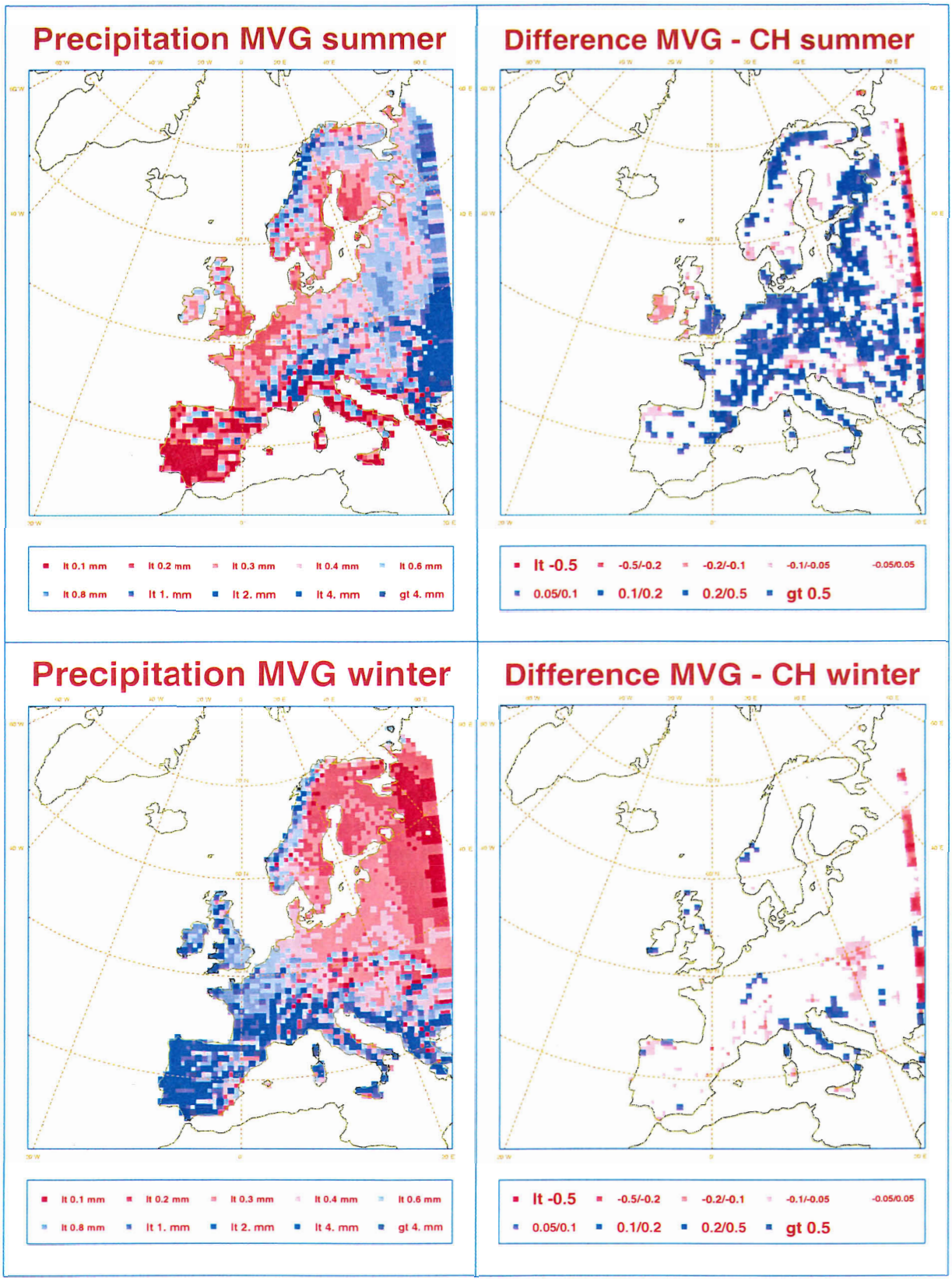

Figure 4.3 (upper charts) Total precipitation averaged for summer (mm per 6 hours) for the MVG run (a) and difference in precipitation between the MVG and CH run (b).

Figure 4.4 (bottom charts) Total precipitation averaged for spring (mm per 6 hours) for the MVG run (a) and difference in precipitation between the MVG and CH runs (b).

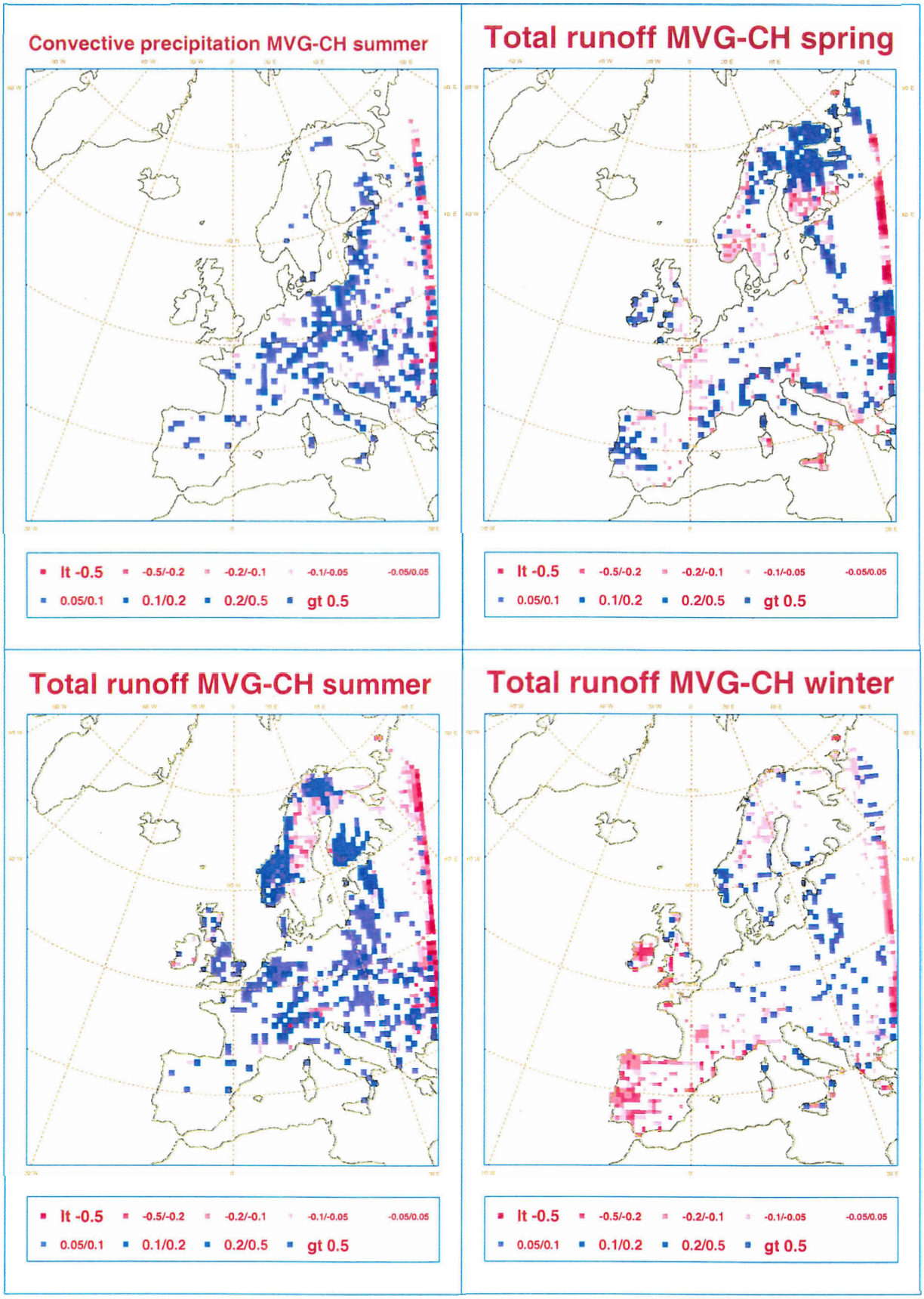

Figure 4.5 (left upper corner) Convective precipitation averaged for summer (mm per 6 hours) for the MVG run.

Figure 4.6 Difference in total runoff (mm per 6 hours) between the MVG and CH runs, averaged for spring, summer and winter.

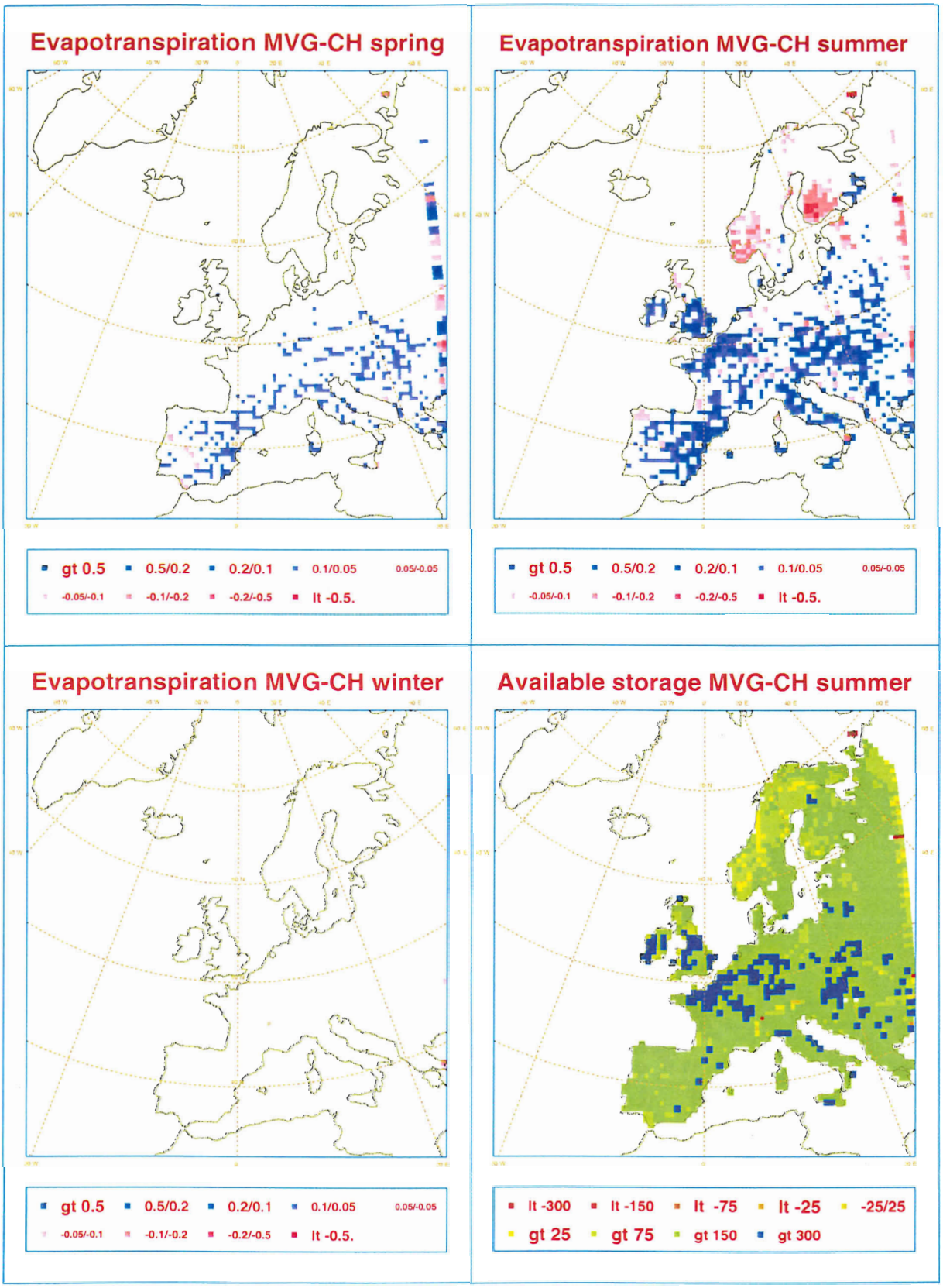

Figure 4.7 Difference in evapotranspiration (mm per 6 hours) between the MVG and CH runs, averaged for spring, summer and winter.

Figure 4.8 (right bottom corner) Difference of available soil water storage (in mm water table) for evaporation and runoff between the MVG and CH runs, averaged for summer.

Figures 4.3 to 4.9 display the spatial distribution for P, R, E and the storage available for evaporation and runoff. The plots of the differences between MVG and CH are highlighted as they explain most changes in water balance terms distribution for the soil texture classes. They support the results from the accumulated time series. The band of gridcells in the east of each plot is caused by disturbance from the model boundary. Differences between MVG and CH runs of more than 0.05 mm per 6 hours (ca. 20 mm per season $\approx$ 10 % of seasonal P) are considered as significant.

4.4.1 Precipitation, runoff and evapotranspiration

Precipitation (large scale and convective)

Figure 4.3 a and 4.4 a show that patterns of total precipitation (P) occur in resemblance with the climate types, described in Chapter 2. Western atlantic coast- and mountain areas receive more P during all seasons. South Europe shows the typical characteristics of the Mediterranean climate with lots of rain in winter and dry conditions in summer. Seasonal averages range from less than 0.1 mm / 6h to more than 2 mm /6 h (resp. 36 mm and 720 mm for a whole season).
Precipitation for MVG parameterization (P_{MVG}) has not changed significantly in comparison to CH parameterization for winter (see figure 4.4 b). In summer however, P_{MVG} is larger than P_{CH} over parts of Central and East Europe with a difference up to 0.2 mm / 6h (figure 4.3 b).
The contribution of convective precipitation (P_c) is only relevant in summer for the continental part of Europe (figure 4.5). Then, $P_{c\text{-}MVG}$ is larger than $P_{c\text{-}CH}$ for almost whole Central and East Europe. The increase of P is observed as a sudden shift in the accumulated budgets for area 2 and 5 (figure 4.2 c and f). In winter, P_c is high for Spain and other regions of South Europe, but no difference between MVG and CH occurs.

Runoff (total and surface runoff)

In spring 1995, the difference of the total runoff (R) for MVG and CH parameterization is distributed in a very variable pattern across Central and South Europe (see figure 4.6). Locally the difference is very high, up to -0.5 mm / 6h (180 mm in total), while positive difference is smaller but more large scaled. Averaged for Europe, there is a small negative difference of ca. 10 mm over the whole season (see budget area 0, figure 4.2 a). For the MVG run however, there is no significant connection between a soil texture and shifts of R. The contribution of surface runoff (R_s), especially during snow melting, is much larger for MVG, due to the lower hydraulic conductivity. This is shown by the positive difference in North Sweden, Finland and parts of Russia. For the coarse texture areas (Norway and South Finland), surface runoff seems to be decreased.
During summer and autumn, R is negligible over South and Central Europe, apart from the mountain areas. R_s is increased, but doesn't affect the accumulated budgets of runoff much. The 'coarse' soils show positive difference, caused by their larger hydraulic conductivity. As the contribution of snow melting to R_s has ended, the 'medium' soils in Sweden (area 3) have negative $R_{MVG} - R_{CH}$.
When P increases in winter over South Europe (Spain, area 4), a strong negative difference in R (up to 100 mm), demonstrated in figure 4.6 c. This is demonstrated in the accumulated budget of area 4 (Figure 4.2 e), by the sudden shift in R after the sharp increase of P.

Evapotranspiration

Figure 4.7 shows the difference in E for the MVG and CH runs ($E_{MVG} - E_{CH}$) for spring, summer, and winter. E_{MVG} increases in comparison to E_{CH} in South Europe during spring 1995. This difference is more than 0.1 mm per 6 hours (ca. 36 mm for the whole season) for some gridpoints. Absolute E is also highest in South Europe (ca. 0.5 mm / 6 h).
When soil moisture storage decreases during summer, the area of highest absolute E moves northwards.

$E_{MVG} - E_{CH}$ remains positive over most parts of South and Central Europe. This particularly refers to the areas with medium and medium-fine soil texture, like Spain, France and Central East Europe. In the (wet) coarse texture areas in North Europe, Norway (area 1) and Finland, E_{MVG} is less than E_{CH} .
During autumn and winter 1996, E_{CH} and E_{MVG} both drop below 0.5 mm / 6h and even towards zero for the areas with snowcover. Difference between MVG and CH is not noticeable.

4.4.2 Total available storage and vertical distribution of soil moisture.

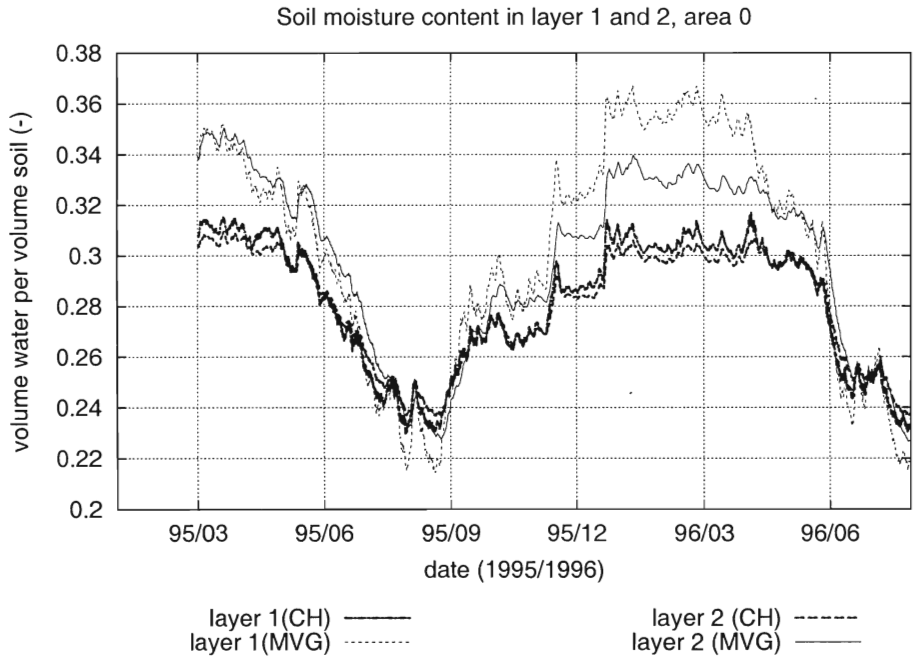

Figure 4.9 a Soil water content for upper soil layers 1 and 2. Shown are the results from the CH run (thick lines) and the MVG run (thin lines).

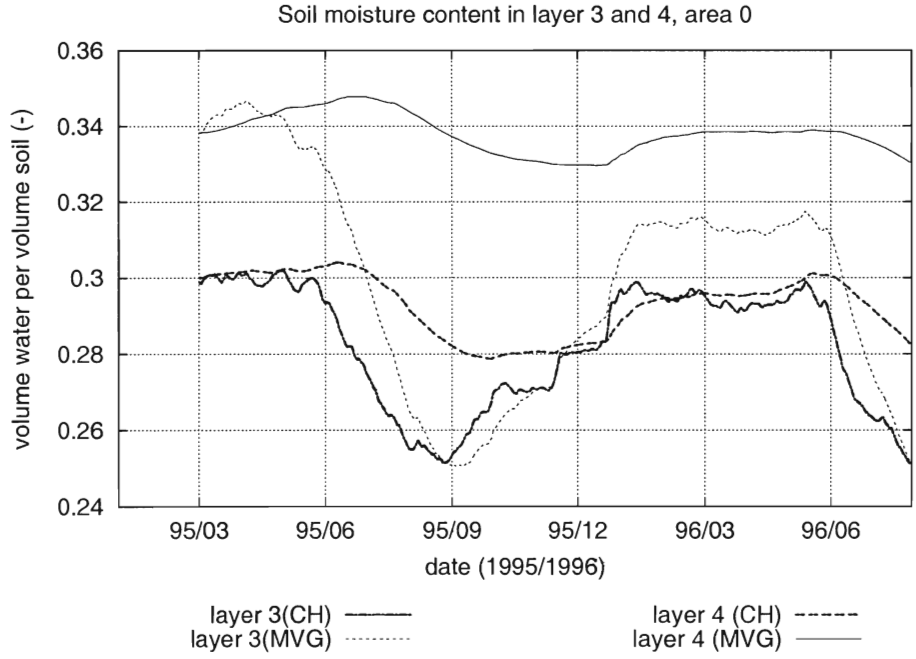

Figure 4.9 b Soil water content for bottom soil layers 3 and 4. Shown are the results from the CH run (thick lines) and the MVG run (thin lines).

Figure 4.8 shows the change of total *available* soil water storage (S), the sum of all four soil layers. This is W_s minus the 'storage' of θ_{pwp} ($= \Sigma (\theta - \theta_{pwp})*B$). Changes in storage indicate how much water has been evaporated, or percolated as deep runoff. The storage in layers 1, 2 and 3 will be used for evapotranspiration, as almost all plant roots are situated there. The majority of the storage is in the thickest layer 4 (B = 1.89 m). Main part of that storage contributes to the deep runoff.

The maximum storage is found in winter. For all soil textures, net advection of water (P-E) is sufficient to refill the soil reservoir during winter. S_{MVG} and S_{CH} is equal then to the storage at initialisation (March 1995). During summer, S_{MVG} and S_{CH} both decrease for Central and South Europe. At the beginning of autumn, values of θ are minimal in the upper soil layers.

The difference between S_{MVG} and S_{CH} reveals the effect of the MVG soil textures in summer. The areas with coarse soil texture have the smallest increase of S (ca. 25-75 mm), and storage in layers 1, 2 and 3 has even decreased (see figure 4.9). The 'medium' area has more increase of S (> 150 mm). The areas with 'medium-fine', 'fine', 'very fine' and 'histosol' classifications are striking with an increase of more than 300 mm (figure 4.8). The effect of the large S_{MVG} for the fine textured soils is also found in the E_{MVG} in summer (see figure 4.7 b). There is a correlation between S and E, as the canopy resistance for E decreases for high averaged θ, see eq. [3.7].

Vertical distribution of θ and consequences for runoff and evapotranpiration

Figure 4.9 shows the distribution of θ for the upper soil layers 1 and 2 (a), and bottom layers 3 and 4 (b) in Europe (area 0). A common feature is that the change of θ for soil layer 4 (θ - $\theta_{March\ 1995}$) is almost equal for the MVG soil textures, compared to the CH soil. The amplitude of θ for layers 1,2 and 3 is larger (up to ca. 0.1 $m^3\ m^{-3}$) for MVG than CH. This amplitude determines the change in soil water storage ($\Delta W_{s\text{-}layer}$) per soil layer. Particularly for the summer season, $\Delta W_{s\text{-}1,2,3}$ for MVG is more negative than for CH parameterization. This indicates that more water is transpired, as highest density of plant roots is located in those soil layers. Even 'coarse' soils can potentially transpire more water than the CH soil, because $(\theta_{cap} - \theta_{pwp})_{MVG\text{-}coarse} > (\theta_{cap} - \theta_{pwp})_{CH}$, see Table 3.2c. The change of soil water storage ($S_{MVG} - S_{CH}$) for soil layer 4 ($\Delta W_{s\text{-}4}$) is less negative in summer, which compensates the effect of $\Delta W_{s\text{-}1,2,3}$. Therefore, the accumulated budgets (figure 4.2) show no distinct negative or positive shift of ΔW_s for all soil layers. The accumulated deep runoff from layer 4 doesn't increase however, due to the lower hydraulic conductivity for the MVG soil textures (except for 'coarse').

4.5 Point validation: comparing model runoff and measurements at Cabauw in 1995 and 1996

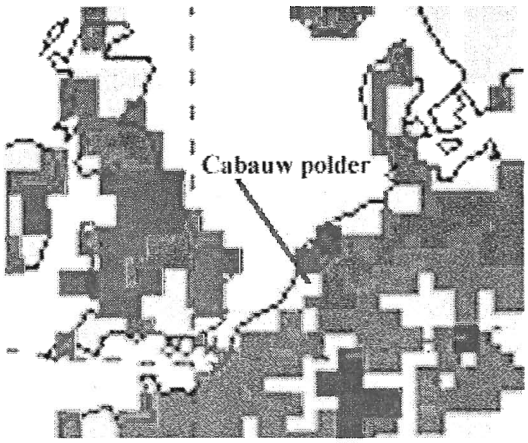

Figure 4.10 Location Cabauw polder and corresponding RACMO grid point (medium soil texture)

Data, assumed to be equal to the runoff for the Cabauw polder in the Netherlands, are available for the period 1993-1999 (pers. com. Bosveld, 2000). This provides verification of the runoff at the corresponding RACMO gridpoint for the simulation period. Figure 4.10 shows the location of the polder 'De Koekoek'.

The size of the polder is 6060 ha, which is about 40 times smaller than the RACMO gridpoint (250000 ha). The surrounding area however is assumed to have the same soil hydraulic characteristics as the selected polder. The abundant water of the polder is drained by several water channels via 2 pumps. The

groundwater level in the polder is kept nearly constant during the year. Soil water storage is thus also considered to be constant. Therefore, the amount of water that is pumped away, is comparible to the net advection ($P - E$), roughly equivalent to the runoff (R). Combining the discharge of the pumps and the area of the drained polder, results in the accumulated R over a selected period (in meters water table) for the whole Cabauw polder. P and E have been measured at the KNMI measuring tower at Cabauw.

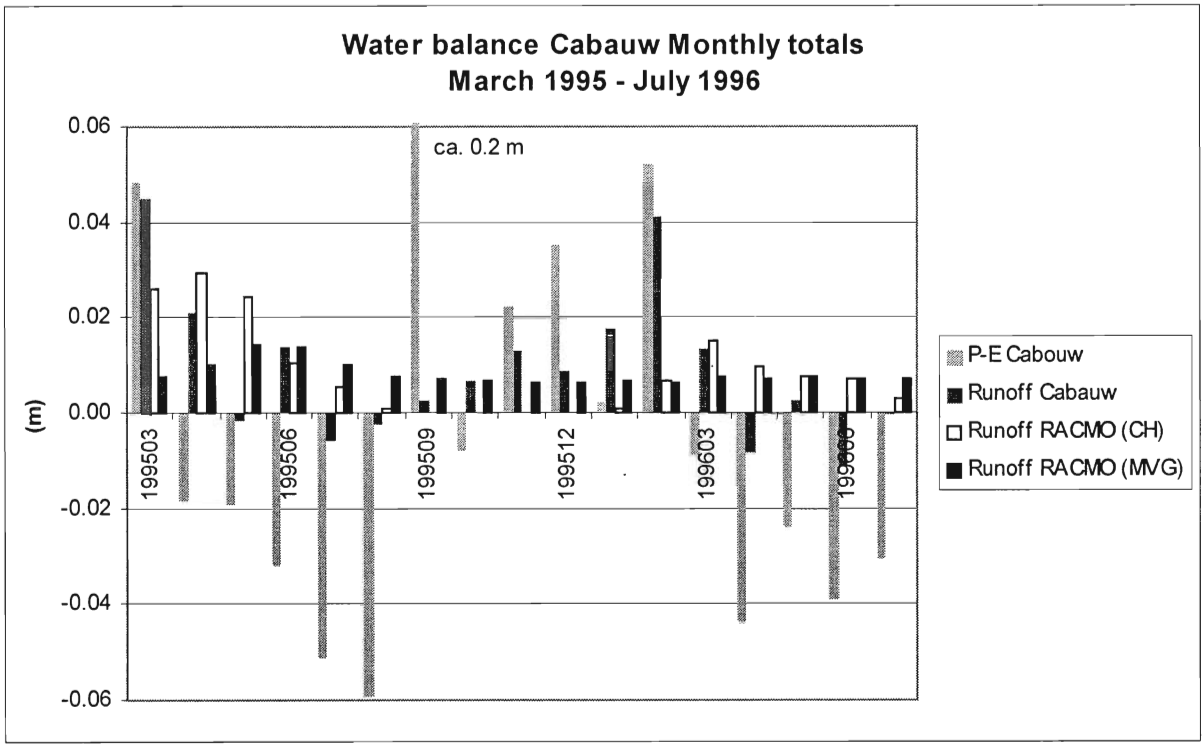

Figure 4.11 Measured runoff at Cabauw polder and the RACMO runoff for the CH and MVG runs

Figure 4.11 displays the results for the simulation period (March 1995 – July 1996). P was very abnormal and variable in that period. After a wet winter in 1995 the net advection (P-E Cabauw) was negative during most months, apart from the extreme event in Sept 1995 (P > 200 mm) and the period November 1995 until February 1996 with positive advection. Total P during March 1995 – March 1996 was 710 mm (normally 750-800 mm), and particularly summer 1995 was very dry. The "measured" R (Runoff Cabauw) shows this. Runoff Cabauw was even negative during May, July and August which means that water had been led into the polder instead of pumped away. The soil dried out anyway during summer, shown by the very delayed reaction of the R to the P of September 1995. Difference between P-E and Runoff Cabauw is relatively large in dry conditions.

The respons of the modelled R for the Clapp and Hornberger (Runoff RACMO (CH)) and Mualem-van Genuchten (Runoff RACMO (MVG)) runs is even slower than Runoff Cabauw.

After initialisation, during March and April 1995, Runoff RACMO (CH) is roughly the same as Runoff Cabauw. After that period, relative differences between the model and the observations are large. During summer and autumn, no R occurs in both the Runoff RACMO (CH) and Runoff Cabauw series. Only after February 1996, Runoff RACMO (CH) becomes significant again. The results for Runoff RACMO (MVG) are even less comparable to the measured R than Runoff RACMO (CH). The peaks of measured runoff are not observed in Runoff RACMO (MVG) at all, and R is distributed more evenly over all months. The presence of summer R for the MVG run, caused by larger θ_{MVG} than θ_{CH} in the bottom layer, is not realistic.

The difference between the modelled and measured runoff may be caused by the next restrictions:

- 'Averaged' hydraulic conductivity for the Cabauw polder is larger than for the model soil, due to the presence of fast draining trenches and ditches. Moreover, there is more surface runoff at the cultivated land (roads, buildings) than the model soil.
- Further, RACMO doesn't take into account the presence of a shallow groundwater table and seepage as a contribution to the runoff. Model boundary conditions are not adequate thus.
- Errors in measured (flux-profile) precipitation and evapotranspiration, up to 10 %, (pers. com. Bosveld, 2000) cause large relative errors in advection when its absolute value is small. Moreover, the frequency of extreme precipitation events differs between the model and the observations

The difference between the modelled runoff for MVG and CH is probably due to the small hydraulic conductivity and larger storage capacity for the MVG soil texture 'medium' compared to the CH soil. That filters out the variability of the advection and decreases and smoothens the runoff output.

4.6 Discussion and conclusions

Precipitation is hardly influenced by MVG parameterization for Europe in total (§ 4.3). In summer, however, both large scale and particularly convective precipitation have increased over large areas of continental Europe (§ 4.4) for the Mualem-van Genuchten run. This may indicate an intensified land circulation of evapotranspiration and precipitation (more E generates more P) over the mainland of Europe, caused by an increased availability of water for all MVG soil textures.

Total runoff, averaged for whole Europe, didn't change significantly. Surface runoff occurs more frequently for all soil textures, except 'coarse', due to the smaller hydraulic conductivity in comparison to CH soil parameterization. Deep runoff has decreased in general during dry conditions (summer and autumn). Reason for that is the increase of water extraction (evapotranspiration) from the upper soil layers in summer. Moreover, the small hydraulic conductivity prevents fast percolation from the bottom model layer.

Evapotranspiration for the MVG run (E_{MVG}) decreases in comparison to E_{CH} for soil texture 'coarse' in North Europe (area 1), during the summer season of the regarded simulation period. The relative small hydraulic conductivity ensures faster percolation. For the 'coarse' soil texture in other regions (area 2) E_{MVG} doesn't differ significantly from E_{CH}. The rest of the soil textures have more E_{MVG} than E_{CH} in spring and summer, caused by the relative small hydraulic conductivity and increased range between θ_{cap} and θ_{pwp}.

Total change of soil water storage has increased ($\Delta W_{s\ MVG}$ is more negative than $\Delta W_{s\ CH}$) or has remained unchanged in summer for almost all soil texture classes. There are no clear relations between ΔW_s and a certain soil texture class, however. Total absolute available storage for evapotranspiration and runoff has increased for all soil textures. Based on the results for runoff and evapotranspiration, a division between soil texture '**coarse**' in wet conditions and the other **finer textures** can be made.
The plots of spatial distribution of evapotranspiration for 'coarse', show that relative more water is 'used' for runoff than for evapotranspiration. For the other (finer) soil textures, the inverse situation occurs. The increased amplitude of θ in soil layers 1, 2 and 3 shows that the (a) soil moisture reservoir has been increased, and (b) the dynamics of runoff and evapotranspiration are intensified.

Verification of the model runoff by measurement at the Cabauw polder shows that the model soil reacts slower on precipitation surplus than the real soil. Differences between the model parameterization and the real physics of the Cabauw polder however are too large for sound assessing of the model results. The effect of changed hydraulic conductivity and storage capacity for MVG and CH parameterization is noticeable.

Skipping all details, the next statements about the relation between distribution of water balance terms and the implementation of the variable soil texture field in summer can be made:

- 'Coarse texture' areas with $k_{MVG} > k_{CH}$ have more runoff and less evapotranspiration, while the change of soil water storage and precipitation doesn't change systematically. These differences are most distinct in wet conditions.
- Soil classes 'medium', 'medium-fine', 'fine/very fine' and the histosols with $k_{MVG} < k_{CH}$ have less or unchanged runoff. Surface runoff increases and deep runoff decreases. Both precipitation - particularly convective - and evapotranspiration increase. Amplitude of soil water storage in the bottom layers increases.

Chapter 5 Comparison of modelled and observed relative humidity

5.1 Introduction

Until now, only the hydrological aspects from the modification in TESSEL has been regarded. This chapter introduces the link to the meteorology, particularly addressing the exchange of water and energy between the land surface and the boundary layer. As shown in chapter 3, the evapotranspiration is a key parameter for the interaction between the energy and water balances.
The shift in evapotranspiration should be verified by observations of latent heat flux (L_vE) which are available for a few sites that had been used for extensive measuring campaigns. Unfortunely, these data cannot be regarded representative for the whole RACMO grid in Europe.
An indirect way to obtain an indication for the change of evapotranspiration (E) between the MVG and CH soil field is analyzing the routinely observed relative humidity (RH) at 2 meter level. This parameter is dependent on the absolute moisture content in the atmosphere, the specific humidity (Q) and the air temperature (T) at 2 m, which determines the maximum Q ($RH \approx Q/Q_{max}$). When more water evaporates from the surface, T is expected to decrease, because more solar energy is used for latent heat energy at the cost of sensible heat energy (Bowen ratio H/L_vE decreases), which decreases Q_{max}. A positive shift of RH thus probably indicates an increase of E, although it is only qualitative in this research. Changes of E, T and Q modify the boundary layer development which has feedback on these parameters. This feedback has not been analyzed, and no exact relation between RH and E will be used. Synops data for Q and T and the dewpoint temperature (D) were available for this research. RH is calculated by T and D using the psychrometer relation. The selection and processing of these data is discussed in § 5.2. In the rest of this chapter, time series from bias and (unbiased) RMS of RH, Q and T for the regional study areas are analysed (§ 5.3). Spatial distribution of RH, Q and T, averaged per season (§ 5.4) will complete the analysis.

5.2 Selection of regional study areas

For the time series, the same areas as used for the water balance study have been selected (see figure 4.2). The grid for analyzing RH, Q and T is based on the available observations. The RACMO grid values are interpolated bilinearly to the spatial positions of the observations. Together with the observed data, they are put into a single file. The density of synops stations differs across Europe and some areas may lack sufficient data. Therefore, it was not possible to choose the gridpoints with only the desired soil texture for the water balance studies for the study areas.

Before a sound statistical comparison between the model and the observed values could be done, obviously unreliable data had to be removed from the observation list. A filtering procedure was based on upper and lower limits for Q, T and D. If data for Q, T and D do not satisfy the selection criteria, the corresponding station codes were put into a **blacklist**. See Appendix C for the exact black listing criteria. During the statistical processing of the time series and spatial analysis, this blacklist is used to exclude unreliable data.

5.3 Statistics for time-series of relative humidity: observed and RACMO values

Figure 5.1 shows the time-series for the observed RH and the model output for MVG and CH, concerning total Europe (area 0). The annual amplitude of the observed relative humidity (RH_{obs}) and the modelled relative humidity (RH_{CH} and RH_{CH}) is ca. 30 %. The upper limit is ca. 90 % for all areas, while the bottom limit varies from 50 % in Mediterranean region to 60-65 % in the rest of Europe.
In April 1996, RH_{obs} is relatively low (< 60 %), caused by low values for area 2 and 5 (<50 %, not shown here). Unreliable synops (dewpoint) data from Germany, which have not been filtered out, may be the

reason of this extreme minimum. The major disadvantage of applying fixed criteria for Q, T and D, is that unrealistic shifts between two time intervals (e.g. 20 ° K within 6 hours) may not be recognized.
The position of the extremes for both model versions is the same during most time; there is thus almost no phase shift between RH_{MVG} and RH_{CH}. So, in the run of the modified TESSEL version with MVG parameterization, no distinct shifts of large scale weather patterns have occured.

The next statistical quantities have been analyzed:

- Bias. This is the absolute difference between the model (m) output and the observations (o), averaged over a certain period and area
- Unbiased Root Mean Square (RMS). $$RMS = \sqrt{\frac{1}{n}\sum_{1}^{n}(m' - o')^2 - Bias^2}$$

Here, m' and o' are the model and observation values at time step n. The influence of the bias in the variability analysis has been eliminated in the expression for RMS. This indicates how good the model output 'follows' the observations.

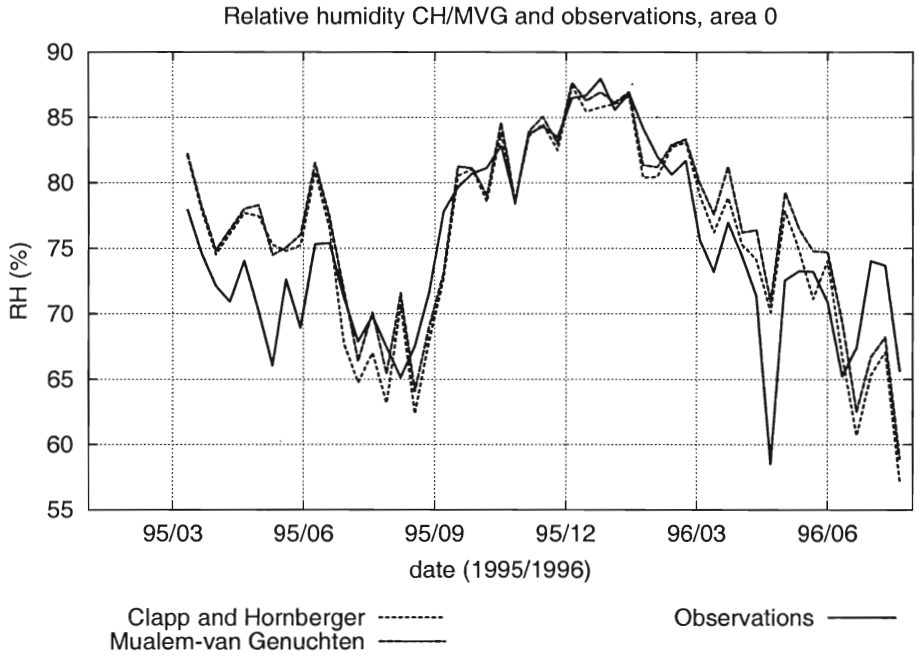

Figure 5.1 Relative humidity at 2 m level (10-day averages). Shown are the time-series of the CH, MVG runs and the observation for the control area 0.

5.3.1 Bias and unbiased RMS for the total control area: Europe

Figure 5.2 a shows the 10-day averaged bias and RMS for Europe (area 0). Both the CH-bias ($RH_{CH} - RH_{obs}$) and the MVG-bias ($RH_{MVG} - RH_{obs}$) are positive in spring and negative in summer. In autumn and winter the bias is almost zero. In general, RH_{MVG} increases, compared to RH_{CH}. This means that the situation declines for spring, but improves in summer.
RMS for MVG run (RMS_{MVG}) is slightly smaller than for CH parameterization (RMS_{CH}). The difference is never significantly (just up to 1 %) There are no indications for a seasonal cycle in RMS_{MVG}-RMS_{CH}. Both RMS_{MVG} and RMS_{CH} reach their maximum in summer due to the more changeable character of the weather.

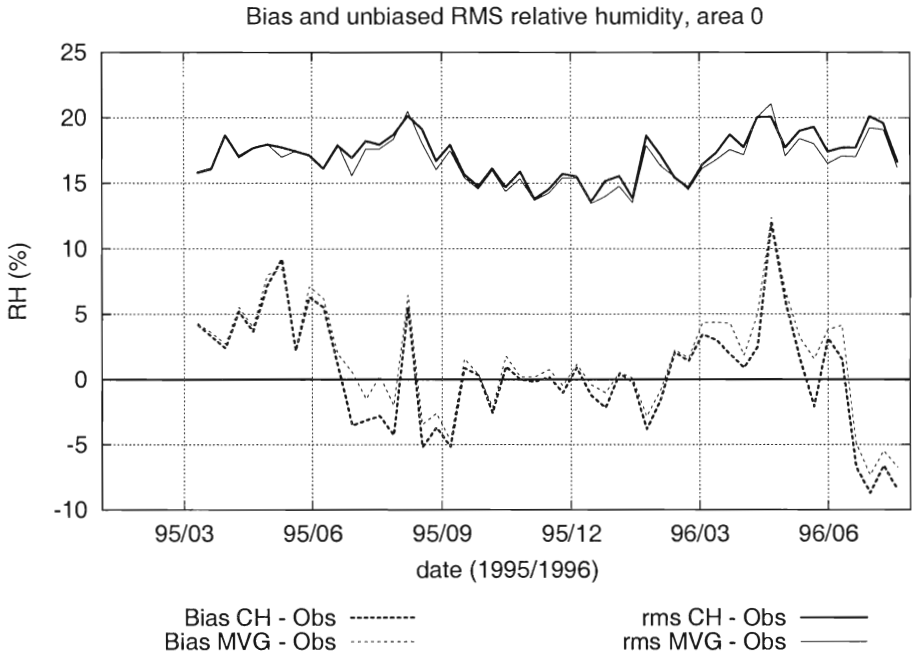

Figure 5.2 a

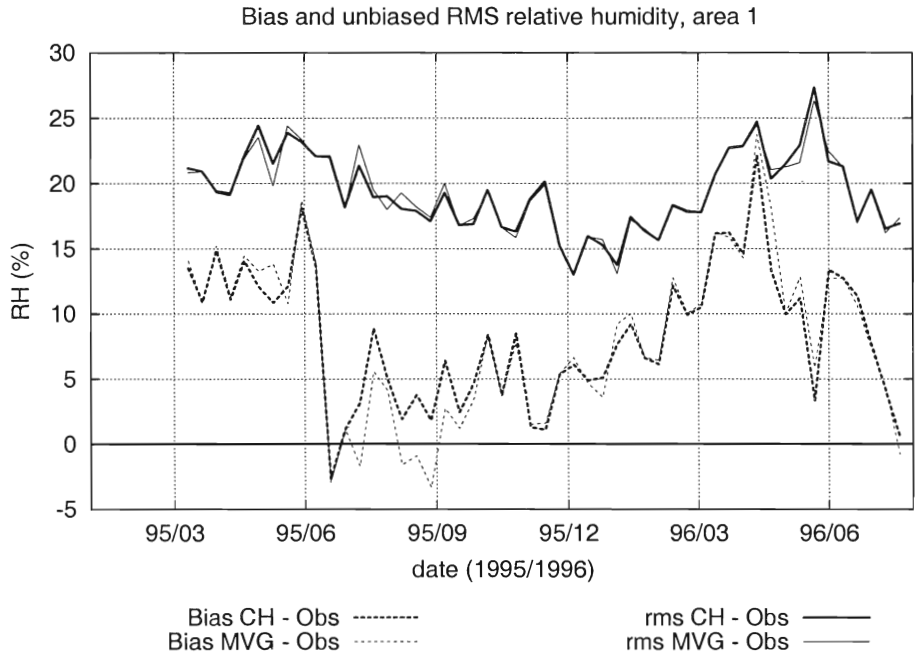

Figure 5.2 b

Figure 5.2 Bias and unbiased RMS of relative humidity at 2 m level (10-day averages). Shown are the time-series for the control area 0 (a), coarse texture area 1 (b), medium texture area 4 (c) and medium-fine texture area 5 (d)

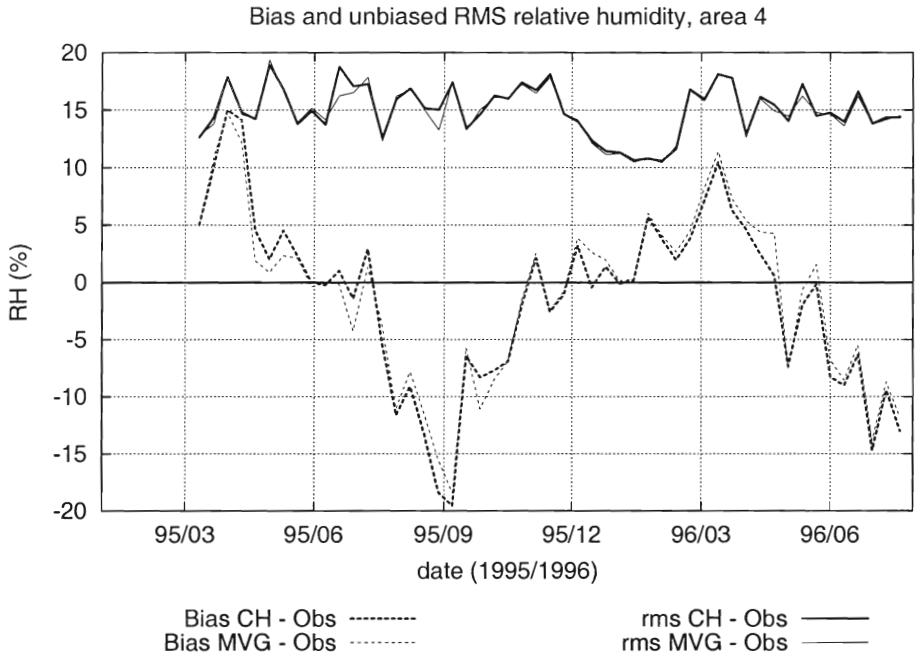

Figure 5.2 c

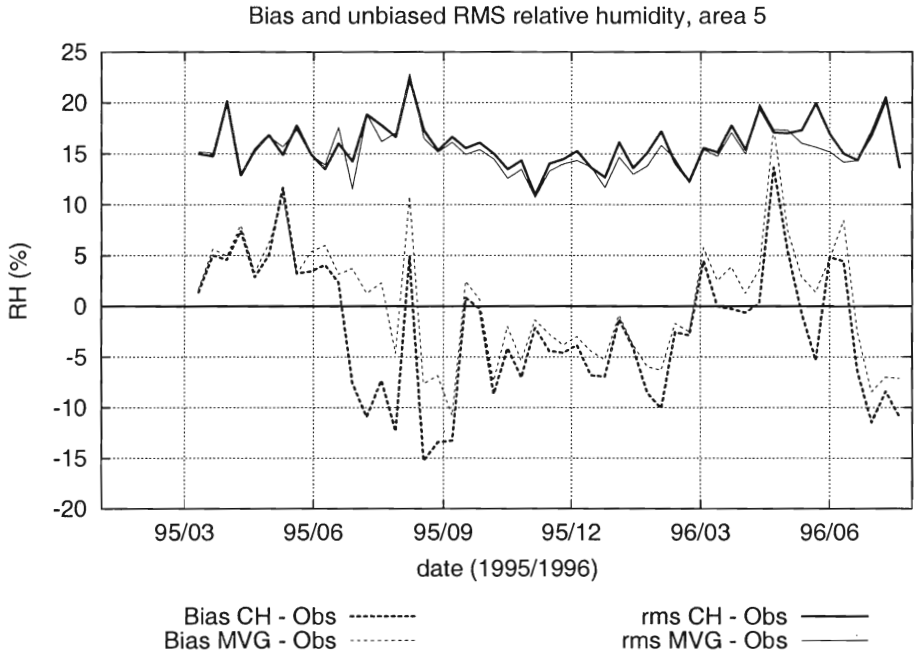

Figure 5.2 d

5.3.2 Bias and unbiased RMS for regional study areas in Europe

The bias for the distinct study areas show the same characteristics as area 0. But areas with high precipitation in the north show an overall positive model bias. Remarkable is that $RH_{MVG} < RH_{CH}$ in summer for area 1 with 'coarse' soil texture, which decreases the model error (Figure 5.2 b). This is also an indication for decreased evaporation at 'coarse' soil texture, shown by the water balance study (figure 4.2 b). For area 2 (Poland), this indication is not pronounced however. Figure 5.2 c (area 4) shows that the medium soil texture areas have not a pronounced difference between RH_{MVG} and RH_{CH}. But the finer texture classes are characterized by a larger RH_{MVG} than RH_{CH}, which is particularly the case for medium-fine area 5 (figure 5.2 d). The fine and histosol areas have the same characteristics as the medium-fine area.

The RMS_{MVG} has been slightly improved for most study areas. RMS_{MVG}-RMS_{CH} is negative during most of the simulation time. There is no region however that has significant smaller RMS_{MVG} as the Europe average (area 0). Area 5 with 'medium-fine' soil texture shows the most pronounced improval for bias and *RMS*.

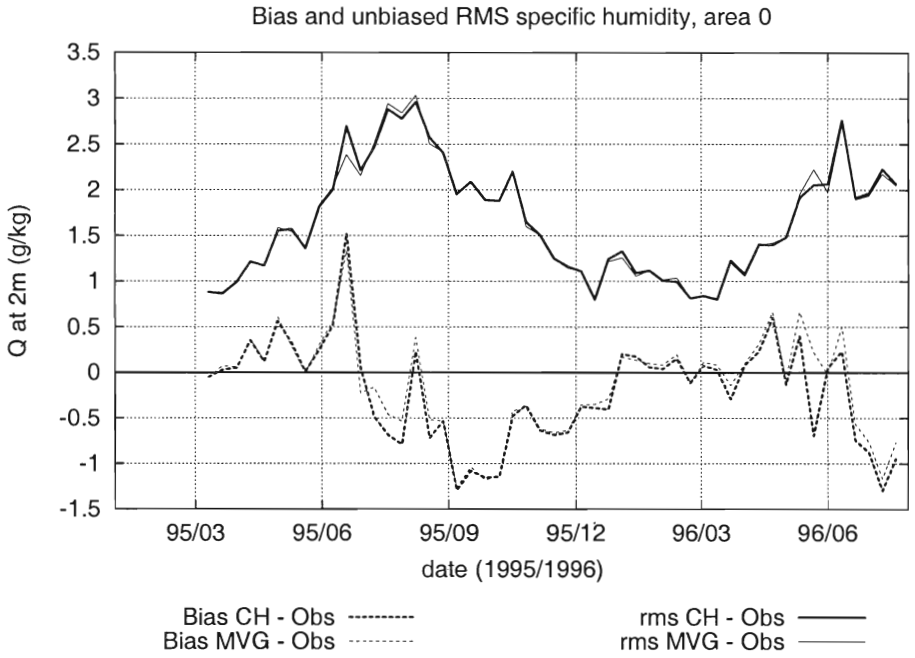

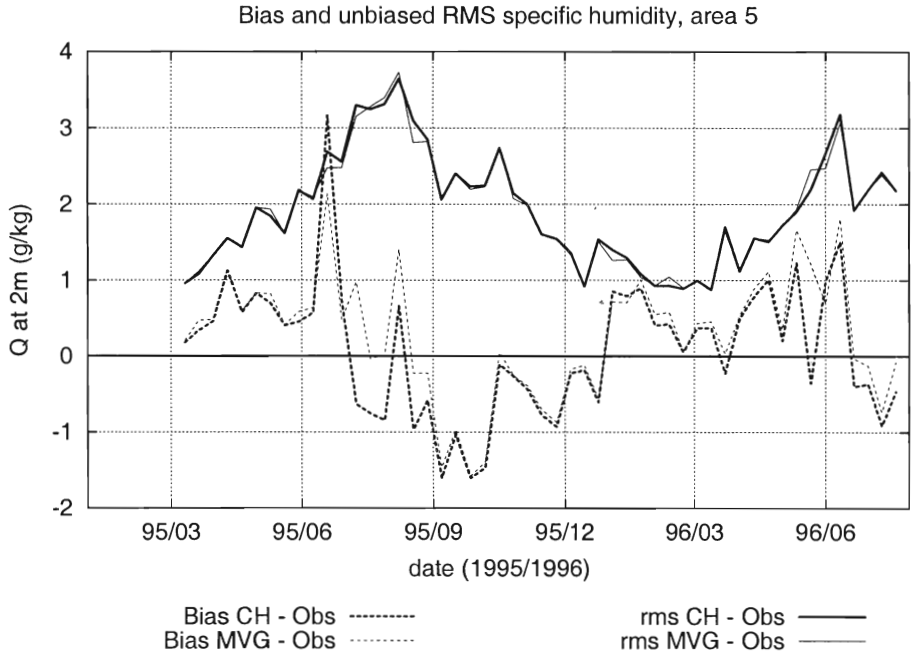

Figure 5.3 Bias and unbiased RMS of specific humidity at 2 m level (10-day averages). Shown are the time-series for the control area 0 (a), and medium-fine texture area 5 (b)

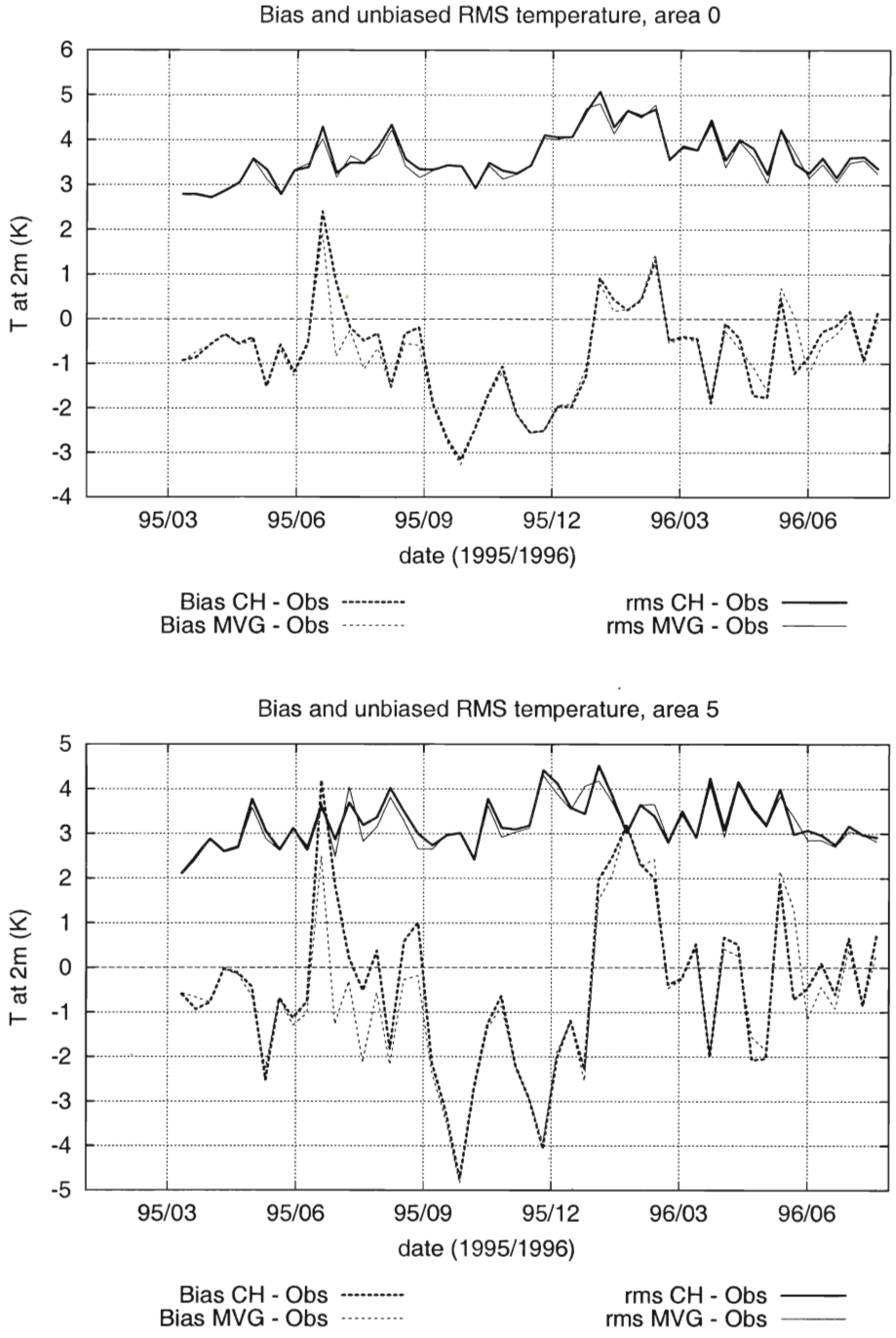

Figure 5.4 Bias and unbiased RMS of temperature at 2 m level (10-day averages). Shown are the time-series for the control area 0 (a), and medium-fine texture area 5 (b)

5.3.3 Statistics for specific humidity and temperature

Specific humidity

The bias of the specific humidity for MVG and CH (Q_{MVG} minus Q_{CH}) is positive, like the bias for the relative humidity, but not as pronounced. For area 0 (figure 5.3 a) and the study areas, the patterns equal those of *RH*. For area 1, Q_{MVG} is less than Q_{CH} , while differences between MVG and CH for area 3 are not significant. Area 5 shows the larger specific humidity in summer for MVG ($Q_{MVG} > Q_{CH}$), resulting in much better model results for Q (figure 5.3 b). In general, the soil textures finer than 'medium' seem to

improve the results for Q in summer.
The difference between RMS_{MVG} and RMS_{CH} is not distinct for neither area 0 or one of the regional study areas. Only area 5 shows systematical decrease of RMS_{MVG}. But anyway, the modified soil parameterization did not decline the results for Q at all.

Adiabatic corrected temperature

Figure 5.4 a and b shows time-series of the bias and RMS for area 0 and 5 respectively.
Averaged for Europe (area 0), both the CH-bias ($T_{CH} - T_{obs}$) and the MVG-bias ($T_{MVG} - T_{obs}$) are negative during most time. In general the bias is not large (up to 3 ° K). The difference between the MVG and CH temperature ($T_{MVG} - T_{CH}$) is not significant. Only during summer, T_{MVG} is smaller than T_{CH} (ca. 0.5 ° K). For the regional study areas, no major shift have been observed either. The strongest shift in summer temperature (1.5 ° K) between the models is found in the medium-fine region, area 5 (Figure 5.4 b).

5.4 Spatial distribution relative humidity and temperature

Relative humidity

Figure 5.5 shows the regional distribution of bias between the model and observed relative humidity ($RH_{CH} - RH_{obs}$ and $RH_{MVG} - RH_{obs}$), averaged for summer and spring. Figure 5.6 shows the difference between the MVG and CH model output ($RH_{MVG} - RH_{CH}$) for summer, autumn, winter and spring.

The negative RH-bias during summer, already indicated by the time series, is evident. Only small parts of Norway and Germany (area 1, 2 and 5) have a positive bias. The MVG soil parameterization decreases the model error (bias) for large parts of Central Europe (figure 5.5). Striking is that RH_{MVG} is particularly lower than RH_{CH} for relatively much gridpoints with 'coarse' soil texture in Norway and Southern Finland (figure 5.6). For the European mainland, $RH_{MVG} - RH_{CH}$ is clearly positive.
In autumn and winter, the negative model bias ($RH_{CH/MVG} - RH_{obs}$) becomes less pronounced for the mainland of Europe. The same happens to the positive difference between RH_{MVG} and RH_{CH}.
In spring, the model-observation bias ($RH_{CH/MVG} - RH_{obs}$) is positive in Central and North Europe (even more than 10 % for Norway). This doesn't improve the model error for that season. The positive bias for Norway occurs in all seasons, while the positive bias for the mainland of Europe is typical in spring (as indicated by the time-series). For Central Europe, $RH_{MVG} - RH_{CH}$ is positive.

As expected, the difference between RH_{MVG} and RH_{CH} runs is particularly pronounced in dry (summer) conditions. For the specific humidity, the same pattern as the relative humidity occurs and will not be discussed in detail.

Adiabatic corrected temperature

Changes in model temperature ($T_{MVG} - T_{CH}$) for summer, autumn, winter and spring) are plotted in figure 5.7. The model bias ($T_{CH/MVG} - T_{obs}$) is distributed very variably over Europe and is mainly caused by flow dynamical influence (not shown).
Summer results show again clearly the difference between the wet coarse areas in North Europe and the mainland of Europe with the other (finer) soil texure classes. T_{MVG} is about 0.1 - 1 ° K *warmer* than T_{CH}, while for the rest of Europe T_{MVG} is 0.1 – 1 ° K *cooler* than T_{CH} with a maximum of 1-2 ° K for the regions with fine and very fine textures. For most grid points, a correlation between T and RH for the coarse and finer soil textures has been observed.
Temperature shifts in winter and spring are less pronounced than in summer. $T_{MVG} - T_{CH}$ for most regions is positive now (0.1 – 1 ° K). The reason for this is unknown.

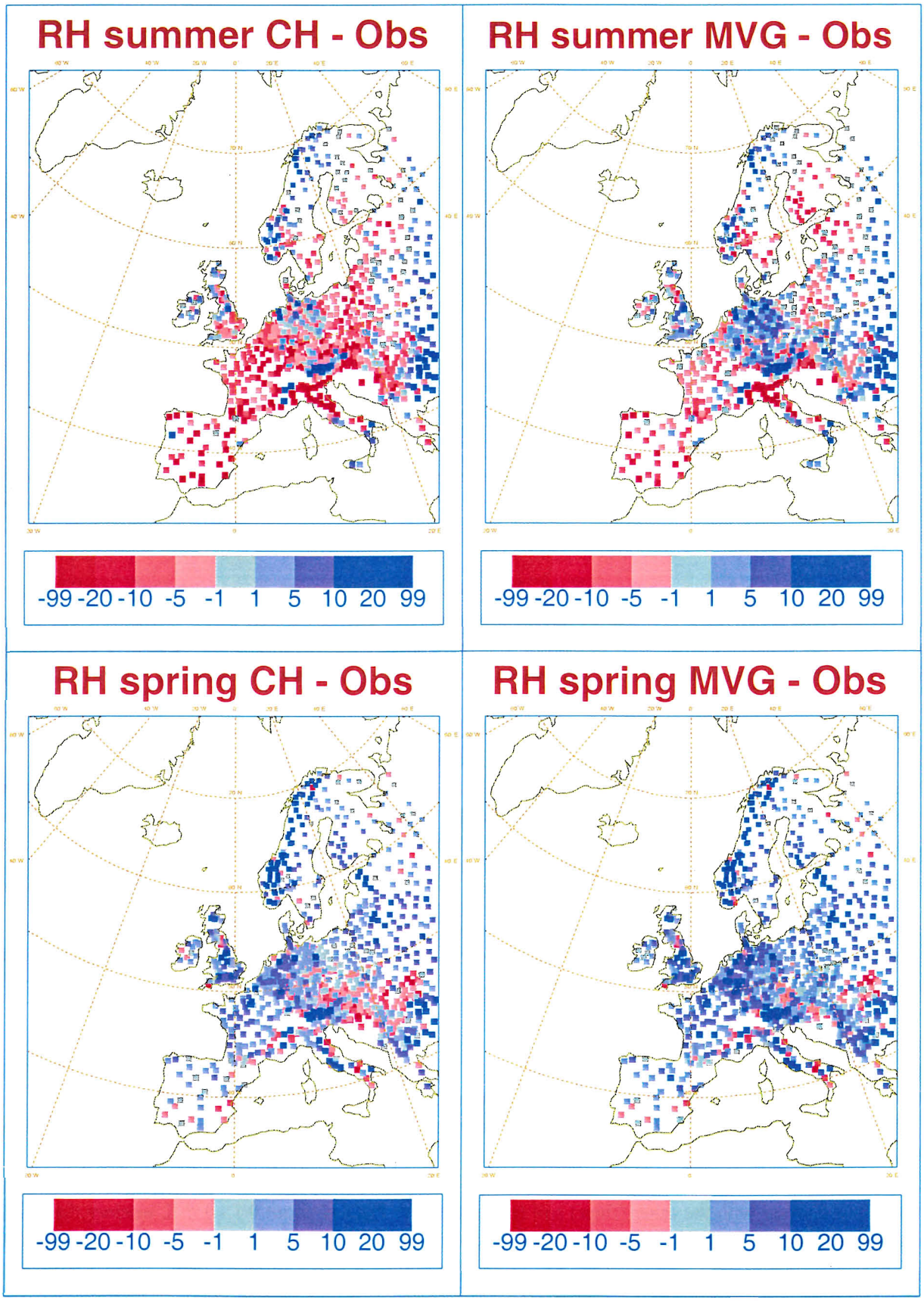

Figure 5.5 Bias of relative humidity (%) between the MVG/CH runs and the observations, averaged for summer and spring.

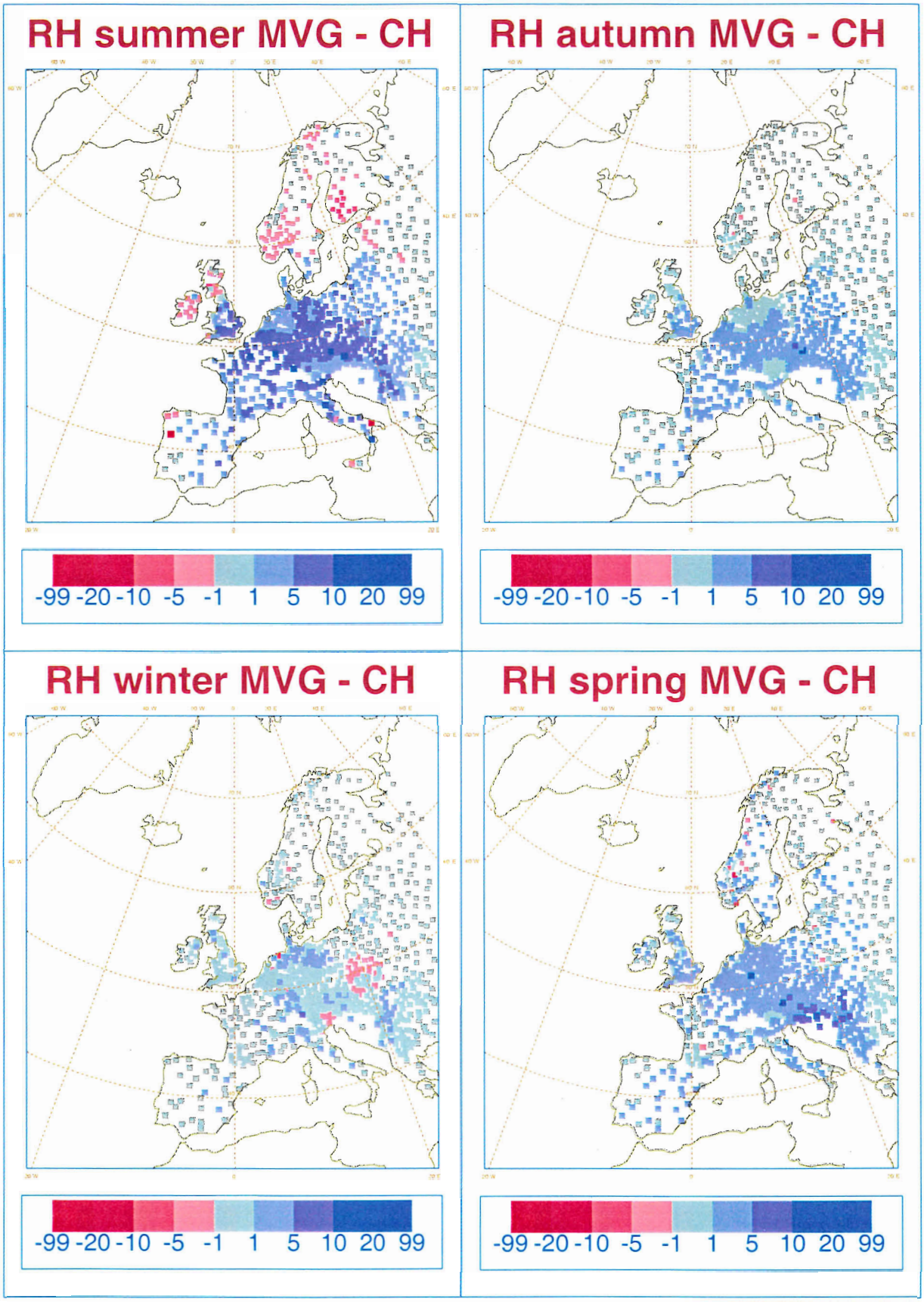

Figure 5.6 Difference of relative humidity at 2 m level (%) between the MVG and CH runs, averaged for summer, autumn, winter and spring.

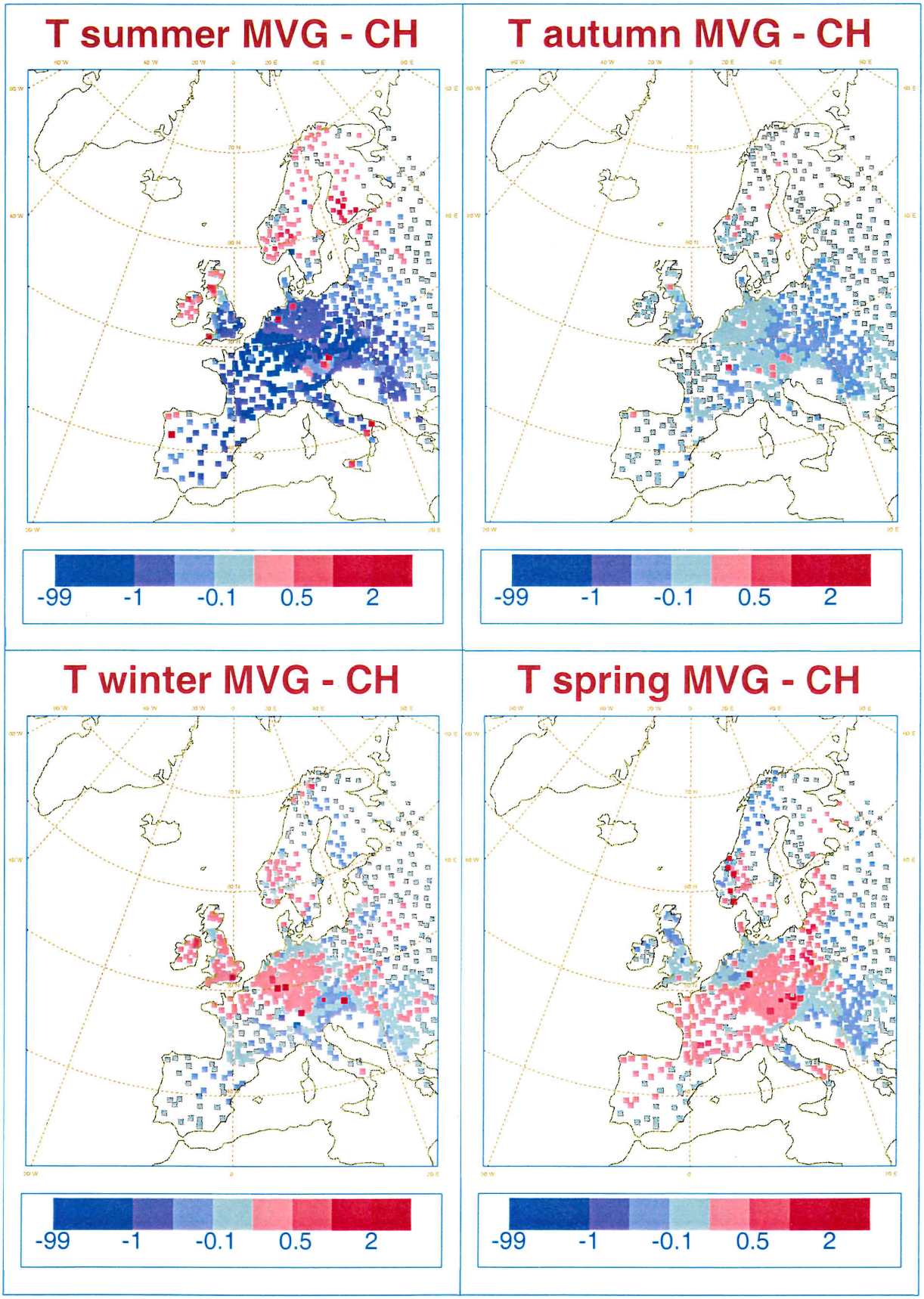

Figure 5.7 Difference of temperature at 2 m level (°K) between the MVG and CH runs, averaged for summer, autumn, winter and spring.

5.5 Discussion and conclusions

For the areas with 'coarse' texture, relative humidity for MVG (RH_{MVG}) has been unchanged or decreased in comparison with RH_{CH}. This generates no improval of the bias model-observations, but it demonstrates the decrease of evapotranspiration in those areas (see figure 4.7). All other (finer) textured soil types show higher RH_{MVG} than RH_{CH} , while evapotranspiration has increased. This indicates a positive correlation between relative humidity and evapotranspiration.

In addition to the conclusions of the relative humidity time series, the maps of ($RH_{MVG} - RH_{CH}$) confirm the positive model-observation bias in spring and negative bias in summer. The influence of the MVG soil textures is not very strong; but a division between smaller RH_{MVG}, linked to smaller E_{MVG} for 'coarse', and larger RH_{MVG} , linked to larger E_{MVG} for the other soil textures in summer can be made.

Analysis of the specific humidity and temperature, particularly in summer, supports the division in relative humidity between 'coarse' and the finer soil textures. Specific humidity increases and temperature decreases in comparison to CH for 'coarse' and decreases and increases resp. for the other soil textures. RMS_{MVG} of specific humidity and temperature is smaller than RMS_{CH}, but the difference is not as significant as for the relative humidity.

The effect of the modified soil parameterization in TESSEL was expected to be highest in dry conditions ($\theta < \theta_{cap}$) during summer, when difference in evapotranspiration are highest too. The results of the relative humidity and temperature confirm this hypothesis.

Chapter 6 Conclusions and recommendations

Conclusions and recommendations about the implementation of a variable European soil map, based on Mualem-van Genuchten parameterization of soil hydraulic properties, are given in this chapter. A systematic overview of conclusions from the soil water balance and relative humidity analyses per soil texture class are summarized in Table 6.1.

6.1 Effect of implementation of variable soil map in RACMO.

- The variable soil map, based on Mualem-van Genuchten parameterization, causes shifts in the modelled water balance terms "precipitation", "evapotranspiration", "runoff" and "change of soil water storage", although they are small.
- A division between coarse soil types and all other fine soil types can be made. Soil type "coarse" has relative large hydraulic conductivity and low evapotranspiration in summer, compared to the Clapp and Hornberger soil type. The other finer soil types have relative small hydraulic conductivity and large soil water storage capacity, which leads to higher evapotranspiration and precipitation on the European mainland in summer.
- Validation of evapotranspiration changes by analyzing observed relative humidity and temperature appears to be successful. Relative humidity increases and temperature decreases in summer as a result of the changes in the soil parameterizations. The average and random model error decreases slightly, particularly in summer.

6.2 Recommendations

- Results from the soil water balance analyses should be validated by observational data, integrated for a certain area. Adequate river runoff data and satellite or remote sensing data for evapotranspiration and precipitation should be available for future research.
- More attention should be paid to adequate filtering of unreliable data from the synops observations in regional climate models, which is the case in operational weather forecast models like HIRLAM.
- Databases, like HYPRES, contain more information about the vertical composition of soils ('horizon' classification) than is currently used by regional climate models. Topsoils and subsoils e.g. can be distinguished. As most landsurface parameterization schemes have more soil layers, this database information could be used to improve the vertical representation of soil hydraulic properties.
- Simulation period for water balance experiments, which is only one year in this research, should be extended to eliminate unwanted effects of the initialisation of e.g. soil water content.
- The effect of land use, like urbanization and water control infrastructure, for modelled water balance should be taken more in account.

Table 6.1 Conclusions concerning the most distinct changes caused by the implementation of the variable soil map, based on Mualem-van Genuchten parameterization, in comparison to the non-variable soil map based on Clapp and Hornberger parameterization.

	Area	Climate type	Soil water balance	Relative humidity (= *RH*)	General conclusions
Europe (total)	0	-	**More** precipitation and evapotranspiration in summer. **More** surface runoff and less deep runoff.	Majority of Europe has **increased** *RH*. Model error[3] decreases, particularly in summer. Temperature decreases in summer, thus Bowen ratio (sensible/latent heat flux) is smaller and evapotranspiration larger.	Small hydraulic conductivity (*k*) and large soil water storage leads to more continental evapotranspiration and precipitation in summer. *RH* and *T* confirm this.
Coarse	1 Norway	Oceanic/Sub-arctic (**wet**)	**More** deep runoff and **less** evapotranspiration in summer	*RH* **decreases** in summer for this area and South Finland. No significant changes occur for the other seasons.	In wet conditions, k is **larger** than the Clapp and Hornberger soil. This leads to **less** evapotranspiration and **more** runoff. Model error for RH and T doesn't decrease much however.
	2 Poland	Continental (**dry**)	More precipitation in summer, and little more evapotranspiration. More deep runoff in wet conditions.	No significant changes occur. *RH* increases at some places due to adjacent medium-fine regions	
Medium	3 Sweden	Sub-arctic (**wet**)	No important changes in precipitation and evapotranspiration. **More** surface runoff in spring, less water storage in soil and thus **less** deep runoff in summer.	No significant changes occur	**More** soil water storage capacity and **smaller** k results in intensification of the mainland circulation of evapotranspiration and (particular convective) precipitation. Annual amplitude of soil water content in the upper soil layers with highest plant root density has increased. Deep runoff decreases, but frequency of surface runoff increases. Enhanced *RH* and lowered *T* for area 5 support the increase of evapotranspiration.
	4 Spain	Mediterranean (**dry**)	**Less** deep runoff in winter and significantly **more** evapotranspiration in summer.	No significant changes occur	
Medium-Fine	5 France/ Germany	Altered Oceanic	**More** convective precipitation and evapotranspiration in summer More deep runoff at field capacity, as hydraulic conductivity is relative large.	RH **increases** in spring, summer and autumn. The model error increases in spring, but decreases in summer. Temperature (*T*) decreases in summer (smaller Bowen ratio). Relative strong decrease of unbiased RMS for both *T* and *RH*.	
Fine + Very Fine	6 Hungary	Continental	Slightly increased summer evapotranspiration and surface runoff	*RH* increases in spring, summer and autumn. *T* decreases in summer and unbiased RMS is smaller, but not as much as for area 5.	Too less data for reliable analysis. Lower hydraulic conductivity and increased storage cause probably more surface runoff and evapotranspiration.
Histosols	7 UK / Ireland	Oceanic	Evidence for more evapotranspiration and less deep runoff in summer.	No significant changes occur; results are not consistent for the whole area.	

[3] Model error is the absolute difference between the model RH (MVG/CH) and the observations.

References

- Betts, A.K., Viterbo, P., and E. Wood, 1998. *Surface energy and water balance for the Arkansas-Red River basin from the ECMWF Reanalysis*. Journal of Climate, vol 11 pp 2881-2897.

- Christensen, J.H., Christensen, O.B., Lopez, P., van Meijgaard, E., and M. Botzet, 1992. *The Hirlam4 Regional Atmospheric Climate Model*. Danish Meteorol. Institute, Copenhagen. Scientific Report 96-4, 51 pp.

- Clapp, R.B. and G.M. Hornberger, 1978. *Emperical equations for some soil hydraulic properties*. Water Resources Journal, no 14, pp 601-604.

- Commissie voor hydrologisch onderzoek TNO (red. J.C. Hooghart), 1986. *Verklarende hydrologische woordenlijst*. Rapporten en nota's no. 16.

- Cosby, B.J., Hornberger, G.M., Clapp, R.B., and T.R. Ginn, 1984. *A statistical exploration of the relation of the soil moisture characteristics to the physical properties of soils*. Water Resources Res, no 20, pp 682-690.

- Cuenca, R.H., Ek, M., and L. Mahrt, 1996. *Impact of soil water property parameterization on atmospheric boundary layer simulation*. Journal of Geophysical Research, Vol. 101, no D3, pp 7269-7277.

- Dolman, A.J. (ed.), 2000. *Representation of the seasonal hydrological cycle in climate and weather prediction models in West Europe*. Interim report NRP project 951246.

- ECSN (European Climate Support Network), Schuurmans, C., and several Co-authors, 1995. *Climate of Europe; recent variation, present state and future prospects*. Published under auspicien of KNMI, The Netherlands.

- Gustafsson, N., 1993. *HIRLAM 2 final report*; available from SMHI, S60-176 Norrköpping, Sweden.

- Henderson-Sellers, A., Yang, Z.L., and R.E. Dickinson, 1993. *The project for Intercomparison of Land-surface parameterization schemes*. Bull. Amer. Meteor. Soc., no 74, pp 1335-1349.

- Jacob, D. and R. Podzun, 1997. *Sensitivity studies with the Regional Climate Model REMO*. Meteorol. Atmos. Physics. 63, pp 119-129.

- Koorevaar, P., Menelik, G., and C. Dirksen, 1983. *Elements of soil physics*. Development in soil science 13. Elsevier Science Publishers.

- Koopmans, R., 1999. Vloeistofmechanica en grondwaterstroming. Collegedictaat nr. 06141005. Wageningen Universiteit, Omgevingswetenschappen.

- Köppen, W. and R. Geiger, 1961. *Die Klimate der Erde*. In: J. Blüthgen, 1966. Algemeine Klimageographie, Walter de Gruyter and Co., Berlin.

- Legates, D.R., and C.J. Willmott, 1990a. *Mean seasonal and spatial variability in global surface air temperature*. In: Theoretical and applied climatology, Vol. 41, no. 1-2, pp 11-21.

- Legates, D.R., and C.J. Willmott, 1990b. *Mean seasonal and spatial variability in gauge-corrected, global precipitation*. In: International journal of climatology, Vol. 10, no. 2, pp 111-128.

- Manabe, S., 1969. *Climate and the ocean circulation*. Part 1: The atmospheric circulation and the hydrology of the earth's surface. Monthly Weather Review, no 97, pp 1-20.

- Shao, Y., and A. Henderson-Sellers, 1996. *Validation of soil moisture simulation in landsurface parameterization schemes with HAPEX data*. Glob. and Plan. Change, no. 13, pp 11-46.

- Roeckner, E., Arpe K., Bengtsson L., Christoph, M., Claussen, M., Dümenil, L., Esch, M., Giorgetta, M., Schlese, U., and U. Schulweida, 1996. *The atmospheric general circulation model ECHAM4: Model descriptio and simulation of present-day climate*. Max-Planck Institute für Meteorologie, Report no 218.

- Van den Hurk, B.J.J.M., Viterbo, P., Beljaars, A., and A.K. Betts, 2000. *Offline validation of the ERA 40 surface scheme*. ECMWF, Technical Memorandum No. 295.

- Van Genuchten, M.T., 1980. *A closed-form equation for predicting the hydraulic conductivity of unsaturated soils*. Soil Science Soc. Am. J., no. 44, pp 892-898.

- Viterbo, P. and A.C.M. Beljaars, 1995. *An improved Land surface parameterization scheme in the ECMWF model and its validation*. J. of Climate, no. 8, pp 2716-2747.

- Warrilow, D.L., Sangster, A.B., and A. Slingo, 1986. *Modelling of land-surface processes and their influence on European climate*. U.K. Met. Office Rep., O20, Tech. Note no.38, 92 pp.

- Wetzel, P.J., Liang, X., Irannejad, P., Boone, A., Noilhan, J., Shao, Y., Skelly, C., Xue, Y., and Z.L. Yang, 1996. *Modeling vadose zone liquid water fluxes: Infiltration, runoff, drainage, interflow*. Global and Planetary Change 13, 57-71.

- Wösten, J.H.M., Lilly, Nemes, A., and C. Le Bas, 1998. *Using existing soil data to derive hydraulic parameters for simulation models in land-use planning*. Report 156 sc-dlo, Wageningen.

- Wösten, J.H.M., Lilly, Nemes, A., and C. Le Bas, 1999. *Development and use of a database of hydraulic properties of European soils*. Geoderma 90, no 3-4, pp 169-185.

Appendix A Background physics of soil hydraulic properties (Koorevaar et al., 1983)

A.1 Potential theory and derivation of pressure head

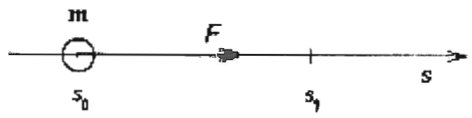

Figure A.1 Mass m moving in the direction of a force field.

In general, when a body with mass m moves over a distance Δs ($s_1 - s_0$) (figure A.1), the system expends an amount of useful work or energy equal to $F^s \Delta s$. The energy lost or gained in these transitions between s_1 and s_0 is the difference in *potential energy* of the mass m in the force field between the two positions. When this difference in potential energy is divided by the mass m, one obtains the potential difference, $\Delta\psi$:

$$\Delta\psi = -\frac{F^s}{m}\Delta s \quad \text{or when } \Delta s \text{ is confined to a infinitesimal distance } ds\text{: } d\psi = -\frac{F^s}{m}ds \qquad [A.1]$$

When choosing a reference position s_0, where $\psi = 0$, the potential for any point s' can be calculated by integrating [A.1]:

$$\psi = -\int_{s_0}^{s'} \frac{F^s}{m} ds \qquad [A.2]$$

Potential is thus potential energy divided by mass and is expressed in J kg^{-1}. The reference point in soil physics and soil studies is generally chosen at the land surface.

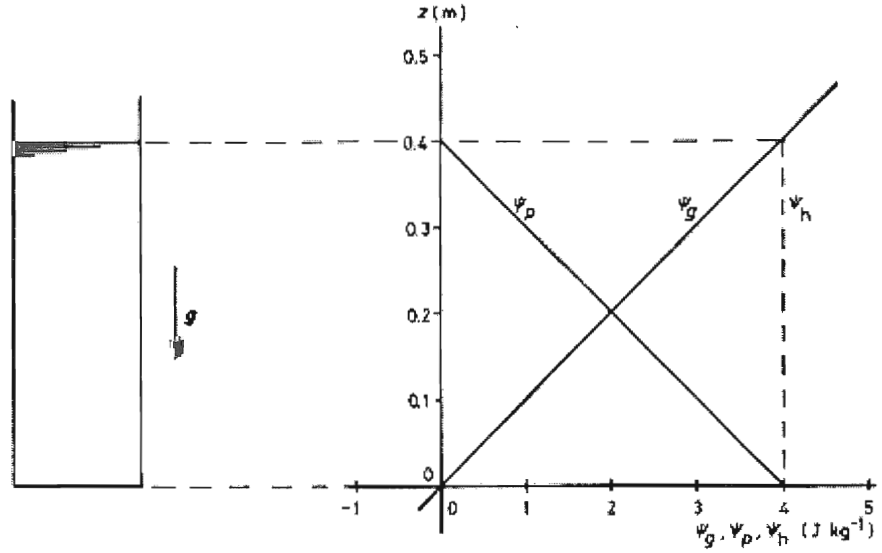

Figure A.2 Column water with gravitational and pressure potential.

Nowthat the potential is introduced, we can discuss the gravitational and pressure potential (from which the pressure head will be derived). Consider Figure A.2, where a column of water is shown at hydrostatic equilibrium in the gravitational field. There is no flow and no work will be done by the gravitational field. So the total potential (ψ_h) is constant. In the gravitational field, the water has a gravitational potential, ψ_g. This leads to:

$$\psi_g = gz + C \qquad [A.3]$$

Usually, the reference for the gravitational potential is chosen such that $\psi_g = 0$ at z = 0, and thereby $C = 0$. Similarly, the pressure potential ψ_p can be formulated, using the hydrostatic pressure relation $dp/dz = -\rho g$,:

$$\psi_p = \frac{1}{\rho_l} p + C \qquad [A.4]$$

Because water is only slightly compressible and its density ρ_l can be regarded as independent of p, we can apply [A.4] for water. The reference for ψ_p is selected at atmospheric pressure, by convention. Then, $\psi_p = 0$ if $p = p_{atm}$. In Figure A.2, the reference for ψ_p is at the water surface, since there is atmosperic pressure. Now the integration constant becomes $-p_{atm}/\rho_l$ which yields:

$$\psi_p = \frac{1}{\rho_l}(p - p_{artm}) = \frac{1}{\rho_l} p' \qquad [A.5]$$

For both hydrostatic and flowing soil moisture, ψ_g and ψ_p are in general the only two components of the total potential that need to be taken into account. The sum of ψ_g and ψ_p is called the hydraulic potential, ψ_h:

$$\psi_h = \psi_g + \psi_p \qquad [A.6]$$

After these theoretical considerations, we now can discuss the pressure head.
The potential can be converted to a potential related to the weight of the soil moisture. Since weight is mg, the potential (J kg^{-1}) has to be divided by g to get the potential on weight basis (J N^{-1}). This formulation is very convenient, because pressure can be related to units of soil depth (m) now. The hydraulic potential [A.6] is converted to the hydraulic head (H):

$$\frac{\psi_h}{g} = H = h + z = \frac{\psi_g}{g} + \frac{\psi_p}{g} \qquad [A.7]$$

Here, z is called the gravitational head and h is the *pressure head*, expressed in meters with the land surface as reference level. So, when h = -1 m, the pressure (relative to atmospheric pressure) of the soil moisture (ρgh) is 1000*9,8*-1 = - 9800 Pa

A.2 flow of water through soils, hydraulic conductivity (k) , diffusivity (D)

Under field conditions, hydrostatic equilibrium almost never occurs. When water flows, there must be a net driving force (ΣF). Divided by mass (m), this is equal to the hydraulic potential gradient:

$$\frac{|\Sigma F|}{m} = -\frac{\partial \psi_h}{\partial s} \quad \text{or divided by weight:} \quad \frac{|\Sigma F|}{mg} = -\frac{\partial H}{\partial s} \qquad [A.8]$$

Now the sum of ψ_g and ψ_p is not constant anymore (see Figure A.3). The minus sign is added to show that the driving force and the flow of water are directed towards the decreasing values of the hydraulic potential. In nature, this hydraulic potential gradient in general is not constant in both space and time most times and the soil is unsaturated. Then *nonsteady flow* in unsaturated soil occurs.
The driving force divided by weight (- ∂H/∂s) will be used from now on.

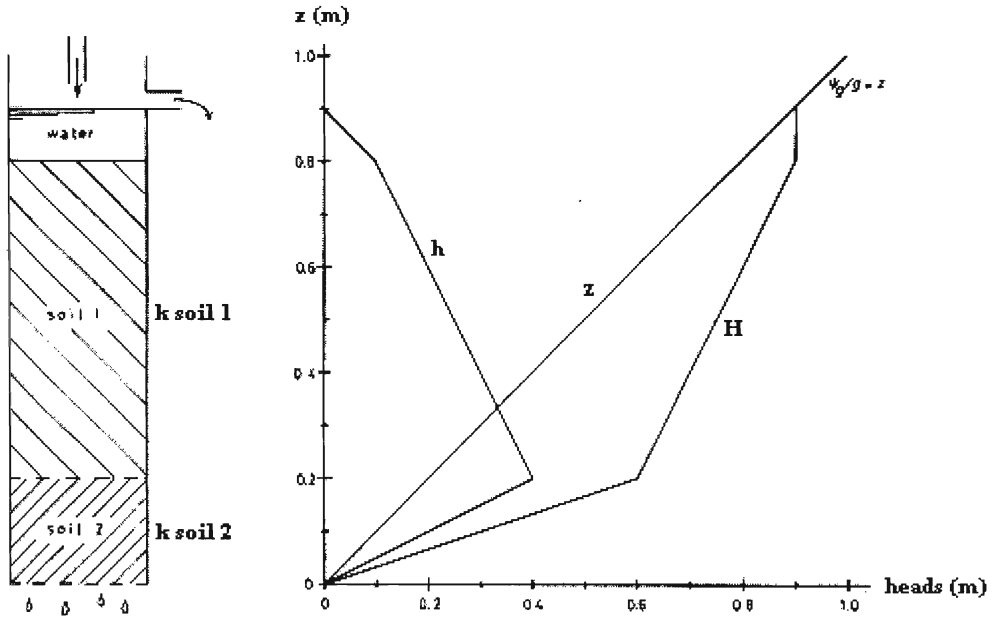

Figure A.3 Laboratory situation with hydraulic potential gradient

For the rate of movement of soil water, the expression 'flux density' is used. This is the amount of water passing through a plane perpendicular to the direction 's' during a time interval, divided by the area of that plane (A) and the duration of the time interval (∂t). This 'flux density' is expressed as a volume (V) and denoted by 'q':

$$q = \frac{\partial V}{\partial t}\frac{1}{\partial A} \quad (\mathrm{m^3\ m^{-2}\ s^{-1}}) \text{ or } (\mathrm{m\ s^{-1}}) \qquad [A.9]$$

Skipping assumptions concerning friction and drag forces, the flux density equation is obtained:

$$q = -k\frac{\partial H}{\partial s} = -k\left(\frac{\partial h}{\partial s} + \frac{\partial z}{\partial s}\right) \qquad [A.10]$$

This is Darcy's law, named after the Frenchman who found this relationship in 1856 when he was experimenting with water in saturated sand.

The proportionality coefficient k is called hydraulic conductivity, as it indicates the ability of the soil to conduct the flow of water. The structure of the soil (texture and stratification of soil layers) and the

viscosity of the water determine k (Koopmans, 1999). In real soils, which are not homogeneous in general, k is thus not constant for all spatial dimensions. In most LSP-schemes, the soil is assumed to be homogeneous.

A basic condition for the transport of water (or energy) is that it obeys the law of conservation. In the soil, we assume that the flow is one-dimensional and temperature doesn't change. Then, the continuity equation can be written as:

$$\frac{\partial \theta}{\partial t} = -\frac{\partial q}{\partial s} + S \qquad \text{[A.11]}$$

In the situation of transport of water in soils, positive and negative accumulation is not only caused by the changes in flux density in the direction of transport. Also local additions to, or extractions from outside the soil layer have to be taken into account. This is represented by the term S in [A.11]. In LSP-schemes this is e.g. local water extraction by plant roots.

To describe the flow of water mathematically, only the flux density equation [A.10] and the continuity equation [A.11] are needed. Now the problem of disclosure arises: The equations have four variables (θ, h, t and s), while s may be composed of up to three coordinates. To reduce the amount of unknown variables, the *differential capacity* is introduced:

$$c = \frac{d\theta}{dh} \qquad \text{and} \qquad D = \frac{k}{c} = k\frac{dh}{d\theta} \qquad \text{[A.12]}$$

Here, D is the diffusivity which is the ratio of k and c. Now, [A.10] can be written as:

$$q = -k\left(\frac{dh}{d\theta}\frac{\partial \theta}{\partial s} + \frac{\partial z}{\partial s}\right) = -D(\theta)\frac{\partial \theta}{\partial s} - k(\theta)\frac{\partial z}{\partial s} \qquad \text{[A.13]}$$

Where the pressure head (h) has been eliminated. D is proportional to the direction of the flux density in opposite direction of the soil moisture gradient and the magnitude of q. Only in homogeneous soils, like in TESSEL, water gradients are also proportional to head gradients .
This flux density equation [A.13] can be substituted in the continuity equation [A.11], obtaining Richards' equation:

$$\frac{\partial \theta}{\partial t} = -\frac{\partial}{\partial s}\left(D(\theta)\frac{\partial \theta}{\partial s}\right) + \frac{\partial}{\partial s}\left(k(\theta)\frac{\partial z}{\partial s}\right) \qquad \text{[A.14]}$$

Appendix B Parameters vegetation tiles

Table B.1 shows the eight tiles and the parameters for the vegetation. Some of this vegetation parameters are discussed at the heat and water balance expressions.

Table B.1 a Eight tiles and some relevant parameters of TESSEL.

Tile	tile class	Parameters
high vegetation	Vegetation	$r_{s,min}$ c_{veg}, LAI, g_D, R, z_{0v},
low vegetation		r_a , r_c / Λ_{sk}, f_R
high veg. with snow beneath	snow/ice	$r_{a,s}$, r_c / Λ_{sk}, f_R
snow on low vegetation		r_a / Λ_{sk}, f_R
sea ice		r_a / Λ_{sk}, f_R
bare ground	bare ground	r_a, r_{soil} r_c / Λ_{sk}, f_R
Interception reservoir	Water	r_a, r_c / Λ_{sk}, f_R
ocean/lakes		r_a / Λ_{sk}, f_R

Table B.1 b Explanation parameters

$r_{a,s}$	Additional aerodynamic resistance to snow (s m^{-1})
r_a	Aerodynamic resistance (s m^{-1})
r_c	Canopy resistance (s m^{-1})
$r_{s,min}$	Minimum canopy resistance (s m^{-1})
c_{veg}	Fraction of vegetation coverage (0..1)
LAI	Leaf area index: area of leaf per area soil (m^2 m^{-2})
g_D	Sensivity coefficient for determining canopy resistance, r_c.
R_s	Percentage of root distribution per soil layer (actually fitting curves) (-)
z_{0v}	Vegetation roughness length (m)
Λ_{sk}	Skin conductivity, determines heat transport from skin layer to soil or snow. Different values for stable and unstable atmospheric boundary layer conditions. (W m^{-2} K^{-1})
f_R	Small fraction of the net shortwave radiation that is directly transmitted to the top soil or snow layer. The remaining part heats up the skin layer. (-)

Λ_{sk}, f_R are present in each tile, the group (r_a , r_c , r_s) refers to a snow resistance scheme, (r_a , r_c) to a canopy resistance scheme and (r_a) to a potential scheme only (see Viterbo et al., 2000).

The transpiration, evaporation from the interception layer and from the bare soil is given by the resistance expression:

$$E = \frac{\rho}{\sum r}\left[Q_a - Q_{sat}(T_0, p_s)\right] \qquad \text{(kg m}^{-2}\text{ s}^{-1}\text{)}$$

Here, Q_a is the specific humidity on surface level and Q_{sat} the saturated specific humidity at the surface temperature (T_0) and air pressure at surface level (p_s). The air density is ρ, and $\sum r$ the sum of resistances, described in table B.2.

Table B.2 Elements of evapotranspiration and pairs of resistances

Evaporation component	sum of r	Description
transpiration	r_a and r_c	Extraction by plant roots, mainly in layers s_1 .. s_3
interception reservoir	r_a (and r_l)	When water storage is not sufficient to evaporate at potential (open water) level, r_l is added. (dependent on potential evaporation in previous timestep)
bare soil	r_a and r_{soil}	Extraction from upper layer only, with soil resistance (r_{soil}) dependent on $\overline{\theta}$, analogue to equation [3.8]. The minimum r_{soil} is 50 s m^{-1}

Appendix C Filtering criteria for blacklist of observed SYNOPS data

The files (sbg-files), generated by the program 'SortBufferGrib' (vdHurk, 1995) contain a datum-time groupe (dtg) culumn and station code column, followed by the parameter data columns. The filtering procedure is based on upper and lower limits for the specific humidity Q, temperature T and dewpoint temperature D, all at standard 2 m observation level. If data for Q, T and D do not satisfy the selection criteria, the corresponding datum-time group plus the station code for RH, Q and T are put into the **blacklist**.

The selection criteria and parameters involved are shown below.

Parameter in blacklist	**Selection criteria**
Specific humidity (Q)	$0 < Q < 50$ (g kg^{-3})
Temperature (T)	$173 < T < 333$ (°K)
Dew point temperature (D)	$173 < D < 333$ (°K)
Relative humidity (RH)	$173 < T < 333$ (°K) **AND** $173 < D < 333$ (°K)

Lay-out:

Lettertype standaardtekst: Times New Roman, pt 11

Editor: word 97
Eindformaat: PDF

KNMI okt 2000